B-cell linker protein prevents aneuploidy by inhibiting cytokinesis

Hiroki Kamino,[1] Manabu Futamura,[1] Yasuyuki Nakamura,[1] Noriaki Kitamura, Koki Kabu and Hirofumi Arakawa[2]

Cancer Medicine and Biophysics Division, National Cancer Center Research Institute, 5-1-1 Tsukiji, Chuo-ku, Tokyo 104-0045, Japan

(Received July 21, 2008/Revised August 14, 2008/Accepted August 15, 2008/Online publication November 19, 2008)

Aneuploidy is a hallmark of human cancers. Although the maintenance of genomic integrity by p53 is important in preventing aneuploidy, its mechanism remains to be elucidated. Here we report evidence that B-cell linker protein (BLNK) mediates the inhibition of cytokinesis, which generates tetraploidy but prevents aneuploidy. We identified BLNK as a transcriptional target of p53. Surprisingly, ectopic expression of exogenous BLNK inhibited cytokinesis, resulting in the formation of tetraploid cells. Indeed, BLNK was involved in the generation of spontaneously arising binucleate tetraploid cells. Interestingly, cytokinesis after DNA damage was inhibited in $p21^{-/-}$ and $p53^{+/+}$ cells, but not in $p53^{-/-}$ cells. BLNK knockdown in $p53^{+/+}$ and $p21^{-/-}$ cells enhanced cytokinesis after DNA damage, leading to the generation of aneuploid cells. In addition, a BLNK-downregulated human pre-B leukemia cell line showed increased cytokinesis and aneuploidy after DNA damage compared with two other pre-B leukemia cell lines expressing higher levels of BLNK. These results suggest that BLNK acts as a mediator of p53 in the inhibition of cytokinesis, which prevents aneuploidy. We propose that the inhibition of cytokinesis is crucial for the maintenance of genomic integrity. (*Cancer Sci* 2008; 99: 2444–2454)

The tumor suppressor p53 prevents malignant transformation when cells suffer stresses including severe DNA damage.[1] Hence, p53 is known as 'a guardian of the human genome',[2] Indeed, p53 is mutated in more than 50% of all human cancers, emphasizing its essential role in tumorigenesis in any of the human cancers. The p53 gene encodes a transcription factor that binds to a specific sequence of its downstream target gene. Therefore, p53 exerts its functions via transcriptional activation of various target genes. Although four major genes, including those functioning in cell-cycle arrest, apoptosis, DNA repair, and antiangiogenesis, are considered to be involved in the core mechanism of p53-regulated tumor suppression, a considerable number of target genes have been reported and their functions display great diversity, implying that many p53-target genes still remains unknown.[3,4] Because the maintenance of genomic integrity by p53 is critical in preventing aneuploidy,[5,6] identification of the p53-target genes involved in this function is important.

Aneuploidy is a major characteristic of various human cancers.[7] Therefore, aneuploidy likely plays a significant role in cancer initiation and progression.[8] There are several checkpoint systems to prevent aneuploidy in normal cells, which monitor proper chromosome segregation, cytokinesis, and cell-cycle progression. Recently, the p53-regulated tetraploidy checkpoint was reported to prevent the progression of aneuploidy.[9–12] At this checkpoint, most cells that suffer from DNA damage progress to mitosis without cytokinesis and arrest at G_1 phase of the cell cycle.[12] Therefore, the arrested cells with DNA damage become tetraploid at G_1 phase. If the function of p53 is impaired, the tetraploid cells at G_1 begin to progress through the cell cycle, replicate DNA, and continue cell division, resulting in the progression of aneuploidy. Although p21/WAF1 has been shown to play a critical role in this checkpoint pathway,[12] the precise mechanism remains to be elucidated.

B-cell linker protein (BLNK),[13] also called SLP-65[14] or B-cell adaptor containing SH2 domain protein (BASH),[15] is a B-cell adaptor molecule and plays an essential role in signal transduction from pre-B-cell receptor and B-cell antigen receptor. As BLNK encodes no intrinsic enzymatic activity, its function is to serve as a scaffold for assembling molecular complexes.[16] After phosphorylation by the kinase Syk, BLNK couples enzymes (phospholipase C, γ2, and Vav) and additional linker proteins (Grb2 and Nck), and regulates downstream signaling pathways.[13–15] The important function of BLNK has been demonstrated by the phenotype of BLNK-deficient mice, which show an incomplete block in B-cell development at the pre-B-cell and immature B-cell stage, suggesting that BLNK is essential for mature development of B cells.[17] More importantly, the BLNK-deficient mice have a high incidence of spontaneous pre-B-cell lymphoma, which likely results from the enhanced proliferative capacity of BLNK-deficient pre-B cells.[18] Consistent with this finding, approximately 50% of human childhood pre-B acute lymphoblastic leukemias show complete loss or drastic reduction of BLNK expression.[19] Those results provide evidence that BLNK acts as a tumor suppressor.[18–20]

Cytokinesis is the physical process by which a cell divides after the completion of mitosis.[21,22] Cell division is completed through the sequential coordination of chromosome segregation and cytokinesis. Mitosis without cytokinesis can produce multinucleate polyploid cells. Cytokinesis at the wrong location and time can lead to the generation of aneuploid cells or mitotic catastrophe. However, despite its importance in cell growth and division, little attention has been paid to the role of the inhibition of cytokinesis in tumorigenesis. Here we report on a cytokinesis-blocking role of BLNK, which is a candidate tumor-suppressor gene in pre-B-cell leukemia. In addition, BLNK-regulated cytokinesis inhibition appears to be involved in the p53-regulated maintenance of genomic integrity, which prevents aneuploidy. We therefore propose that cytokinesis block is an essential safeguard system that prevents aneuploidy arising from cell division with chromosome missegregation and breakage or DNA damage.

Materials and Methods

Detection of binucleate cells. Various HDK1 and HMEC4 cells, including parental, GFPsi, BLNKsi-1 (si-1), BLNKsi-2 (si-2), and BLNKsi-3 (si-3) cells, were seeded in six-well plates at a density of 1.5×10^5 or 2×10^5 cells/plate, respectively. After 72

[1]These authors contributed equally to this work.
[2]To whom correspondence should be addressed. E-mail: harakawa@ncc.go.jp

doi: 10.1111/j.1349-7006.2008.00990.x
© 2008 Japanese Cancer Association

(HDK1) or 24 h (HMEC4), we randomly captured up to 50 fields of vision, each of which included approximately 20 cells, as photographic images using an Olympus IX71 microscope and DP70-BSW software (Olympus, Tokyo, Japan). The numbers of mononucleate, binucleate, and multinucleate cells were counted in approximately 500–600 independent cells. The ratio of the binucleate cells (including approximately 10% multinucleate cells) to the total number of cells was calculated and evaluated statistically.

Detection of micronucleate cells. Various HCT116-p53$^{+/+}$ or p21$^{-/-}$ cells, including parental, GFPsi, si-1, si-2, and si-3 cells, were seeded in six-well plates at a density of 3×10^5 cells/plate. After 24 h, the cells were treated with 1 μg/mL adriamycin for 2 h. At the indicated times, 25–30 fields of vision, each of which included approximately 20 cells, were captured as photographic images using an Olympus IX71 microscope with DP70-BSW software. The numbers of mononucleate, binucleate, and micronucleate cells were counted in approximately 500 independent cells. The ratio of the mononucleate, binucleate, or micronucleate cells to the total number of cells was calculated and evaluated statistically.

Cytokinesis index. HCT116-p21$^{-/-}$ or HCT116-p21$^{-/-}$-BLNKsi-1 cells were treated with 1 μg/mL adriamycin for 2 h, and then 250–350 independent cells were monitored until 24 h after treatment by time-lapse microscopy. The number of cells that had undergone cytokinesis was counted, and the ratio of the cells that had undergone cytokinesis to the total number of cells was calculated and evaluated statistically.

Fluorescence *in situ* hybridization analysis. To examine aneuploidy with probes specific for chromosomes 8 and 12, CEP8 (30-160008; Abbott Molecular, Des Plaines, IL, USA) and CEP12 (D12Z3, 32-112012; Abbott Molecular) DNA probe kits were used. The cells were fixed in Carnoy's liquid (acetic acid : methanol = 3:1) at room temperature for 30 min. Slide glasses were allowed to dry, and were incubated sequentially in 2× saline-sodium citrate (SCC) and 0.1% Nonidet P-40 (NP-40) at 37°C for 30 min. The slides were then incubated in increasing concentrations of ethanol (70, 85, and 100%) for 1 min each. Then, the slides were incubated in 70% formamide and 2× SSC at 73°C for 5 min, and incubated in increasing concentrations of ethanol (70, 85, and 100%) for 1 min each. The slides were allowed to dry completely, and then 10 μL hybridization solution containing labeled probes at a concentration of 1 ng/μL per probe was added to each slide glass, which was incubated at 42°C for 16 h. The slides were washed three times in 50% formamide and 2× SSC at 45°C for 10 min, and then incubated in 0.1% NP-40 and 2× SSC at 45°C for 5 min. The nuclei on the slides were stained with 4′, 6-diamidino-2-phenylindole (DAPI) II. The chromosome 8 (green) and 12 (red) signals were examined using an Olympus IX71 microscope and DP70-BSW software in 300 independent nuclei to detect aneuploid cells, which were defined as the number cells with zero, one, or three signals of either chromosome 8 or chromosome 12. The ratio of aneuploid cells to the total number of cells was calculated and evaluated statistically.

Results

Identification of BLNK as a novel p53-inducible gene. In order to identify new p53-target genes, we screened p53-inducible genes using microarray analysis, as reported previously.[23] The expression level of BLNK was notably elevated in the hepatoblastoma cell line HepG2 infected with Ad-p53-wt (data not shown). BLNK is an adaptor protein that is involved in B-cell receptor signaling,[13–15] and its role in B-cell tumorigenesis has previously been reported in both human and mouse pre-B leukemias.[18–20] As the expression of BLNK can be induced by p53, we speculated that it might be involved in the tumorigenesis of various cell types in addition to B cells. We therefore further analyzed the activities of BLNK. As indicated in Figure 1a,b, BLNK expression was strongly induced in response to DNA damage in p53 wild-type colorectal cancer cell lines (HCT116-p53$^{+/+}$ and LS174T-control), but the induction of BLNK was severely impaired in the corresponding isogenic p53-deficient cell lines (HCT116-p53$^{-/-}$ and LS174T-p53si). Similar results were obtained in other cancer cell lines, including HepG2 and the breast cancer cell line MCF7 (data not shown). These results suggest that endogenous p53 activates the transcription of BLNK in response to DNA damage in various cell types in addition to B cells.

We identified a possible p53-binding sequence (p53BS) in intron 1 of the BLNK gene (Fig. 1c). A chromatin-immunoprecipitation assay indicated that the DNA fragment containing p53BS was immunoprecipitated with an anti-p53 antibody, and was polymerase chain reaction amplified with the precipitated genomic DNA; this suggested that p53 interacts with p53BS *in vivo* (Fig. 1d). Moreover, a heterologous reporter assay showed that the transcriptional activities of luciferase reporter plasmids containing p53BS (pGL-pro-BS, pGL-promoter 1xBS, and pGL-promoter 2xBS) were strongly enhanced when they were cotransfected with wild-type (WT)-p53 but not mutant (MT)-p53, indicating that p53BS is a p53-responsive sequence of BLNK (Fig. 1d). Based on these findings, we concluded that BLNK is a bona fide target of the tumor suppressor p53.

B-cell linker protein inhibits cytokinesis and induces binucleate tetraploid cells. To explore the function of BLNK as a mediator of p53, we prepared an adenovirus vector containing full-length BLNK complementary DNA (cDNA; Ad-BLNK), which was designed to express the full-length BLNK protein. As indicated in Figure 2a,b, when p53-deficient cells (such as HCT116-p53$^{-/-}$ and HepG2-p53si) were infected with Ad-BLNK, the number of tetraploid cells with 4 N DNA content increased by 24 h. This phenomenon was also observed in the p53-mutated glioblastoma cell line U373MG (Fig. 2c). All of the cell lines infected with Ad-BLNK experienced cell death 48–72 h after infection. These results suggest that the overexpression of BLNK preferentially generates tetraploidy.

To investigate the mechanism of the BLNK-induced tetraploidy, U373MG cells infected with Ad-BLNK were monitored by time-lapse microscopy. Surprisingly, most of the cells infected with Ad-BLNK showed inhibition of cytokinesis, resulting in the generation of tetraploid cells (Fig. 2d). These results suggest that BLNK might be involved in the inhibition of cytokinesis and the generation of tetraploid cells.

The role of BLNK is closely related to the generation of tetraploid cells via cytokinesis block. A previous report showed that chromosome non-disjunction accelerated tetraploid cell formation in order to prevent aneuploidy.[24] According to this model, tetraploid cells could be actively generated by an unknown mechanism in order to stop cell cycle progression of cells with chromosome non-disjunction.[24] We therefore speculated that BLNK might generate tetraploid cells in order to prevent aneuploidy. To validate this model, we inhibited the expression of BLNK with short interfering RNA (siRNA) against the BLNK sequence in normal human dermal keratinocyte (HDK1) cells, which were used previously,[24] as well as in normal human mammary epithelial cells (HMEC4). As shown in Figure 3a,b, the expression of endogenous BLNK mRNA was significantly downregulated in HDK1-si-1, HDK1-si-2, HMEC4-si-1, and HMEC4-si-2 cells. Consistent with these expression levels, BLNK knockdown significantly decreased the number of spontaneously arising binucleate tetraploid cells in these lines (Fig. 3a,b). Our results suggest that BLNK is important in the generation of spontaneously arising binucleate tetraploid cells.

B-cell linker protein is involved in the p53-regulated mononucleate tetraploid checkpoint. Contrary to previous observations,[24] DNA

© 2008 Japanese Cancer Association

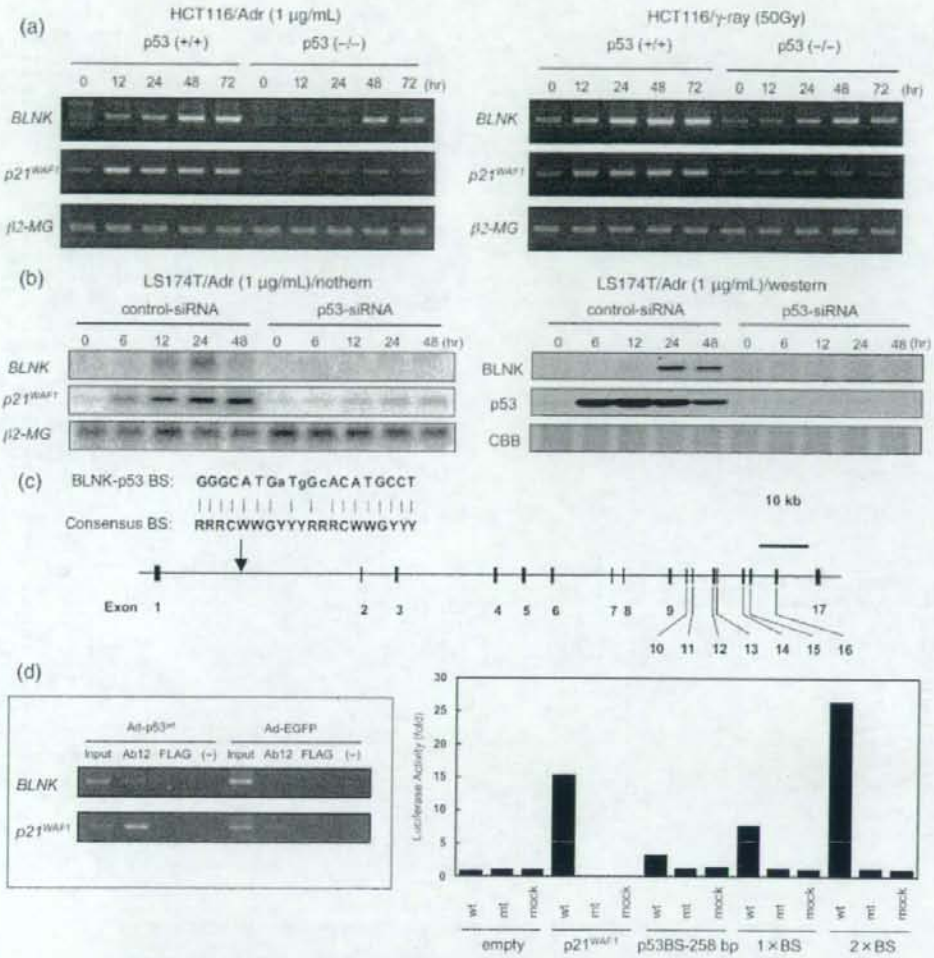

Fig. 1. Identification of B-cell linker protein (BLNK) as a direct target gene of p53. Endogenous p53-dependent induction of BLNK in (a) HCT116-p53$^{+/+}$ and p53$^{-/-}$ cells, or (b) LS174T-control-si and p53-si cells after DNA damage by treatment with 1 μg/mL adriamycin. Expression levels are shown by (a) reverse transcription–polymerase chain reaction, and (b) northern and western blot analysis. Beta 2-microglobulin expression or coomassie brilliant blue (CBB) staining was used as a loading control. p21^{waf1} was used as a positive control. (c) Identification of p53-binding sequence (p53BS) in the genomic DNA of BLNK. Black boxes indicate the locations and relative sizes of 17 exons; the arrow indicates the potential p53BS in intron 1 of *BLNK*. (d) Binding of p53 with p53BS of BLNK and p53-dependent transcriptional activity of p53BS. A chromatin-immunoprecipitation assay was carried out on the DNA–protein complex, which was immunoprecipitated with anti-p53 antibody from HepG2 cells infected with Ad-p53 or Ad-EGFP at a multiplicity of infection of 30. The heterologous luciferase reporter plasmid containing p53BS (258 bp), 1 × BS (20 bp) or 2 × BS (40 bp) was cotransfected with the plasmid designed to express wild-type p53 (wt), mutant p53 (mt), or no p53 (mock) into H1299 cells. The luciferase activity 24 h after transfection is shown in relation to the activity of the pGL3-promoter vectors without p53BS, 1 × BS, or 2 × BS.

damage did not enhance the generation of binucleate tetraploid cells in our current system (Fig. 3c,d). G_1 arrest of the mononucleate tetraploid cells after DNA damage was previously suggested to be involved in a p53-regulated DNA-damage checkpoint that induces long-term cell cycle arrest and subsequent cellular senescence.[25] We therefore proposed that BLNK-induced cytokinesis block might be involved in the DNA-damage checkpoint. Indeed, after DNA damage, the HCT116-p53$^{+/+}$ cells moved from cell cycle phase G_2 to G_1 without cytokinesis, as indicated by decreased cyclin B1 and CDK1 expression, and increased expression of cyclin E, cyclin D, and p27 (Fig. 4a,b). These cells eventually arrested in G_1 phase in the mononucleate tetraploid state until at least 72 h after the DNA damage when some cell death was observed (Fig. 4a,c). By contrast, HCT116-p53$^{-/-}$ cells had a tetraploid DNA content 24 h after DNA damage (Fig. 4a) and cell cycle arrest was not observed, as indicated by increased levels of cyclin B1 and CDK1 expression, and decreased expression of cyclin E, cyclin D, and p27 (Fig. 4b). Eventually, the tetraploid DNA content decreased as a consequence of cell division

doi: 10.1111/j.1349-7006.2008.00990.x
© 2008 Japanese Cancer Association

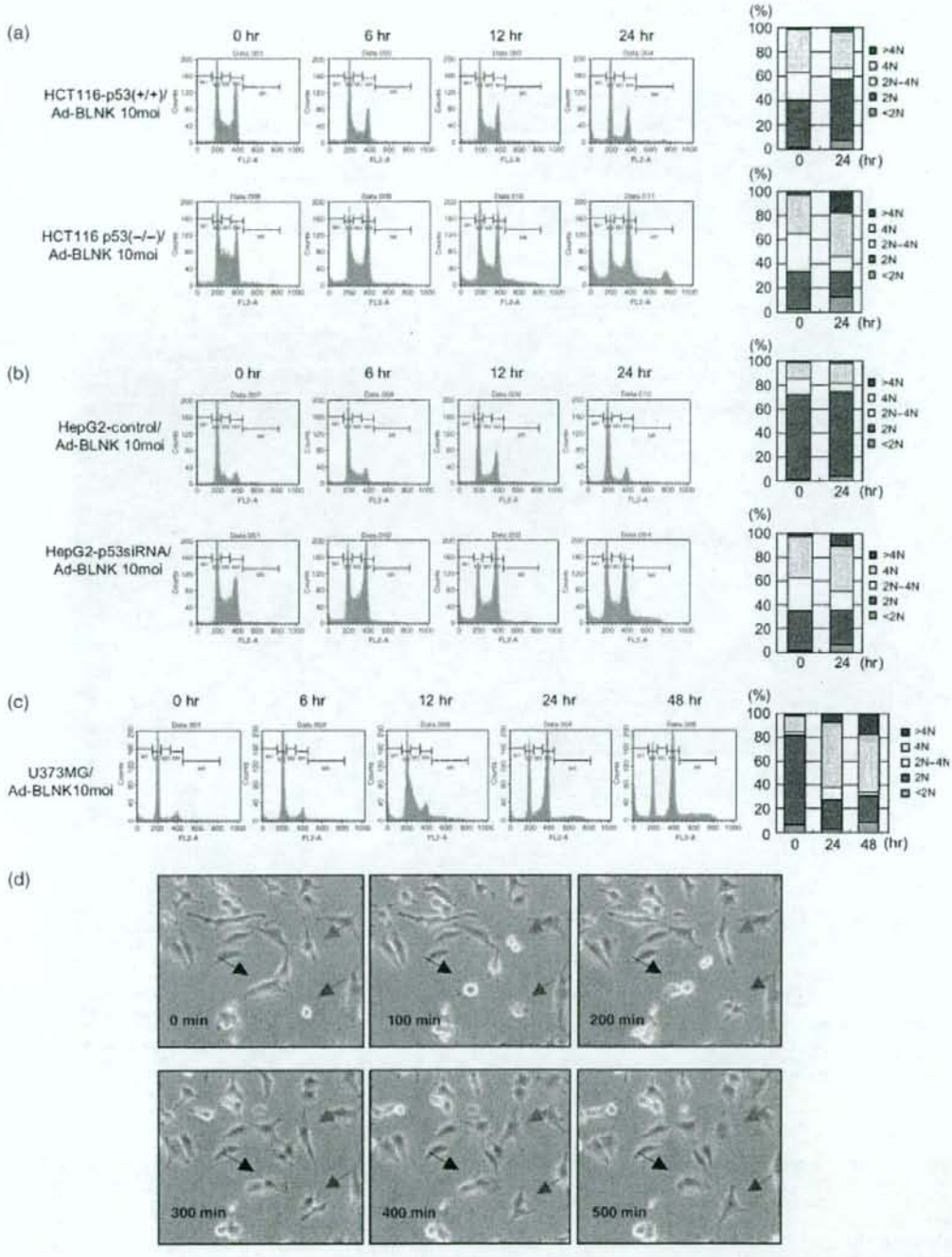

Fig. 2. B-cell linker protein (BLNK) induces binucleate tetraploid cells by inhibiting cytokinesis. (a–c) BLNK induces tetraploidy. p53-wild-type and p53-deficient cancer cell lines, including (a) HCT116-p53$^{+/+}$ and p53$^{-/-}$, (b) HepG2-control and p53si, and (c) U373MG cells were infected with Ad-BLNK at a multiplicity of infection of 10. The DNA contents were examined by fluorescence-activated cell sorting (FACS) analysis at the indicated times. The results are shown as FACS images. (d) BLNK inhibits cytokinesis. A time-lapse microscopic analysis was carried out to monitor the cytokinesis of U373MG cells infected with Ad-BLNK at a multiplicity of infection of 10. Arrows (black, red, blue) indicate the cells that have undergone inhibition of cytokinesis.

© 2008 Japanese Cancer Association

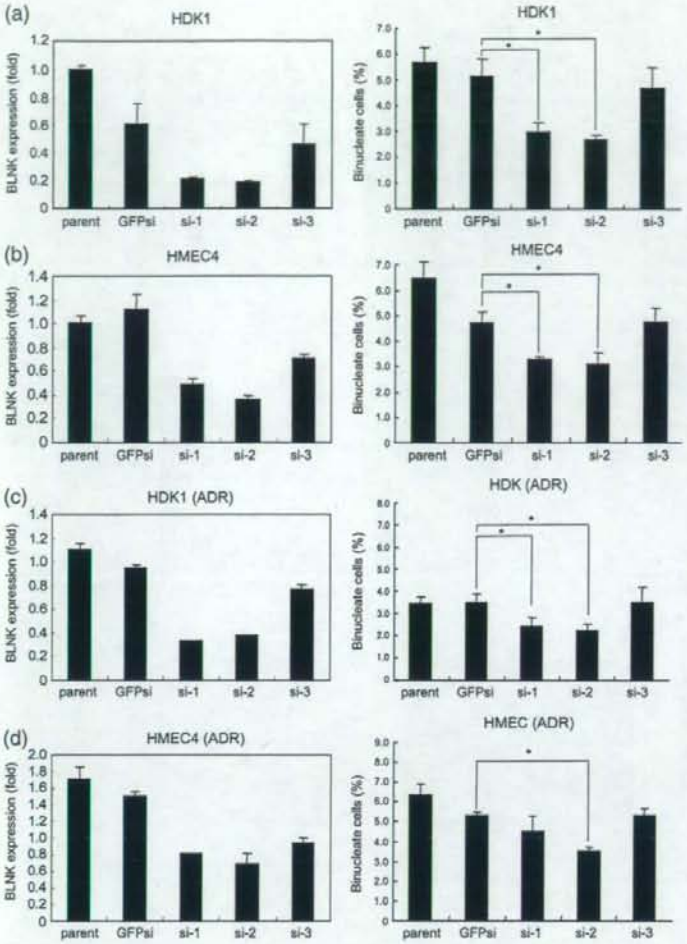

Fig. 3. B-cell linker protein (BLNK) is involved in the generation of spontaneously arising binucleate tetraploid cells. (a,b) Spontaneously arising binucleate tetraploid cells. Downregulation of endogenous BLNK expression by shot interfering RNA (siRNA) in (a) HDK1 or (b) HMEC4 cells. BLNK mRNA was downregulated with three different siRNA: BLNKsi-1 (si-1), BLNKsi-2 (si-2), and BLNKsi-3 (si-3). Parental HDK1 and HMEC4 cells (parent), or HDK1 and HMEC4 cells infected with retrovirus containing the siRNA of green fluorescence protein-si (GFPsi), were used as negative controls. Endogenous BLNK mRNA expression was examined by real-time polymerase chain reaction analysis. BLNK was involved in spontaneously arising binucleate tetraploidy. The numbers of binucleate cells in (a) HDK or (b) HMEC cells, in which BLNK was downregulated with the siRNA of si-1, si-2, and si-3, were counted. Parental HDK and HMEC cells, or HDK and HMEC cells infected with GFPsi siRNA, were used as negative controls. Error bars ± SD ($n = 4$); $^*P < 0.01$, Student's t-test. (c,d) Binucleate tetraploid cells after DNA damage. Endogenous expression levels of BLNK mRNA in various (c) HDK1 or (d) HMEC4 cells after DNA damage. Endogenous BLNK mRNA expression was examined by real-time polymerase chain reaction analysis in parental, control (GFPsi), and BLNK-knockdown (si-1, si-2, and si-3) HDK1 or HMEC4 cells after DNA damage with 1.0 μg/mL adriamycin. DNA damage did not induce the generation of binucleate tetraploid cells. The numbers of binucleate cells in (c) HDK or (d) HMEC cells, in which BLNK was downregulated with si-1, si-2, and si-3 siRNA, were counted after DNA damage by 1.0 μg/mL adriamycin (ADR). Parental HDK and HMEC cells, or HDK and HMEC cells infected with GFPsi siRNA, were used as negative controls. Error bars ± SD ($n = 4$); $^*P < 0.01$, Student's t-test.

leading to aneuploidy or cell death (Fig. 4a). In addition, the cells had abnormal multilobulated nuclei (referred to hereafter as micronucleate cells) as described previously[26] (Fig. 4c). However, the phenotype of the HCT116-p21$^{-/-}$ cells appeared to differ from that of the HCT116-p53$^{-/-}$ cells. In the early phase, similar to the HCT116-p53$^{-/-}$ cells, the HCT116-p21$^{-/-}$ cells became tetraploid by 24 h, and the cell cycle subsequently proceeded with a significant fraction of dead cells (Fig. 4a). However, in contrast to the p53$^{-/-}$ cells, many HCT116-p21$^{-/-}$ cells were not only micronucleate but also relatively large in size, and had a polyploid (>4 N) phenotype 72 h after DNA damage (Fig. 4a,c), implying a failure of cytokinesis. Time-lapse microscopy confirmed that that HCT116-p21$^{-/-}$ cells had entered M phase, but many failed to complete cytokinesis, thereby resulting in endomitosis and a polyploid phenotype (data not shown). We hypothesized that BLNK might contribute to the failure of cytokinesis and the polyploid phenotype in the HCT116-p21$^{-/-}$ cells.

We thus examined the expression levels of p53, p21, and BLNK in these cell lines. As expected, p53 and p21 expression was not detected in HCT116-p53$^{-/-}$ and p21$^{-/-}$ cells, respectively (Fig. 4b). Interestingly, the expression level of BLNK in the HCT116-p21$^{-/-}$ cells was as much as twice that in the HCT116-p53$^{+/+}$ cells (Fig. 4b). Therefore, in order to examine the role of BLNK in cytokinesis inhibition after DNA damage, its expression was downregulated with siRNA against the BLNK sequence (Supporting Fig. S1a,b). As shown in Figure 4d, BLNK knockdown significantly enhanced the generation of micronucleate cells after DNA damage in HCT116-p53$^{+/+}$ and p21$^{-/-}$ cells.

B-cell linker protein prevents aneuploidy by inhibiting cytokinesis. To determine whether the elevation of micronucleate cells was caused by enhanced cytokinesis, we monitored the HCT116-p21$^{-/-}$ parent cells and the BLNK-si-1 cells until 24 h after DNA damage using time-lapse microscopy, and counted the number of cells that completed cytokinesis during this period. As indicated in Figure 5a, BLNK knockdown in the BLNK-si-1 cells enhanced cytokinesis by as much as three times compared with the parental cells, implying that BLNK was involved in the failure of cytokinesis in the HCT116-p21$^{-/-}$ cells. We proposed that the failure of cytokinesis induced by BLNK might prevent

doi: 10.1111/j.1349-7006.2008.00990.x
© 2008 Japanese Cancer Association

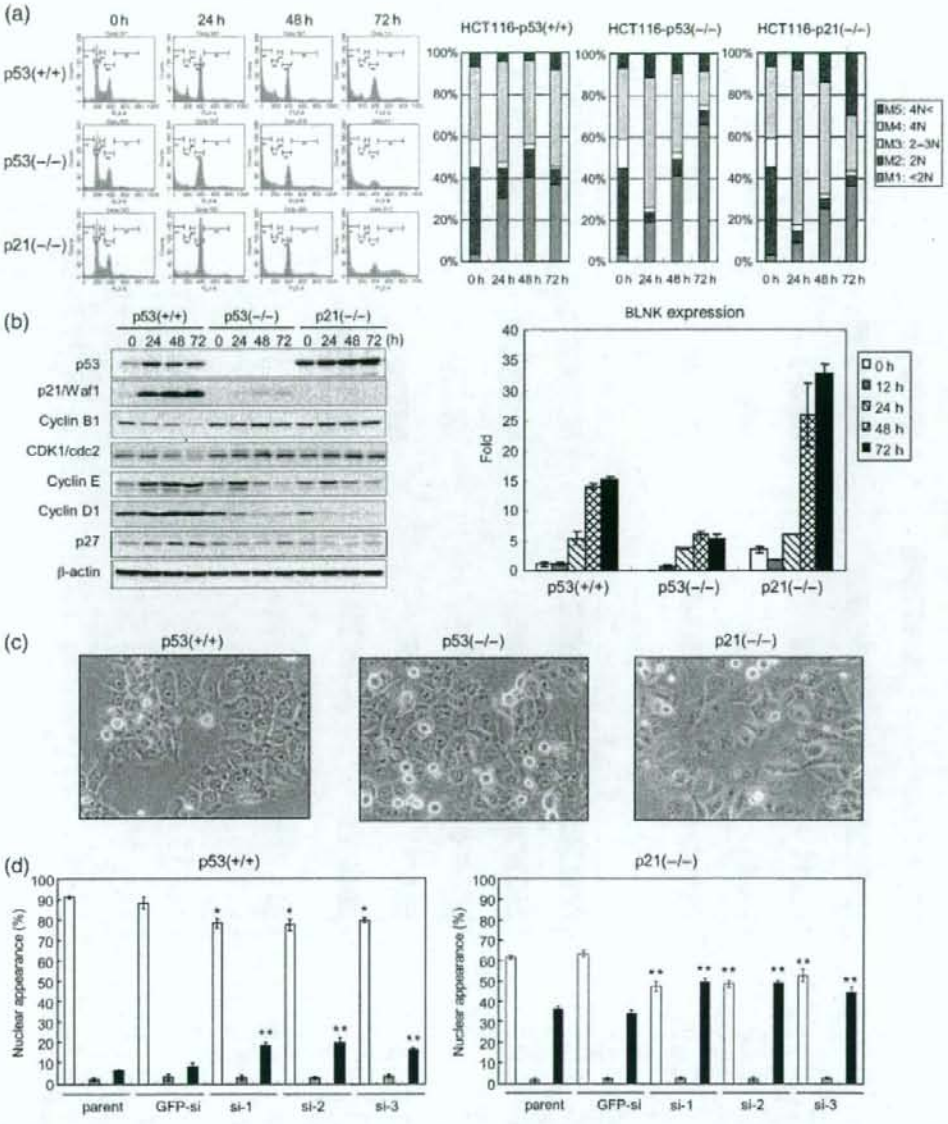

Fig. 4. B-cell linker protein (BLNK) is involved in the p53-regulated mononucleate tetraploid G_1 checkpoint after DNA damage. (a) The DNA contents of HCT116-p53$^{+/+}$, p53$^{-/-}$, and p21$^{-/-}$ cells after DNA damage. HCT116-p53$^{+/+}$, p53$^{-/-}$, and p21$^{-/-}$ cells were treated with 1.0 μg/mL adriamycin, and the DNA contents were analyzed at 0, 24, 48, and 72 h after the treatment, by green fluorescence activated cell sorting (FACS) analysis. The polyploidy phenotype after DNA damage was observed only in HCT116-p21$^{-/-}$ cells: M1 ≤ 2 N; M2 = 2 N; M3 = 2 N–4 N; M4 = 4 N; M5 ≥ 4 N. The results were shown by FACS images (left) and bar graphs (right). (b) Expression levels of various cell cycle regulators and BLNK in HCT116-p53$^{+/+}$, p53$^{-/-}$, and p21$^{-/-}$ cells after DNA damage. HCT116-p53$^{+/+}$, p53$^{-/-}$, and p21$^{-/-}$ cells were treated with 1.0 μg/mL adriamycin, and the expression levels of p53, p21waf1, cyclin B1, CDK1/cdc2, cyclin E, cyclin D1, and p27 were examined by western blot analysis with specific antibodies at the times indicated. β-Actin was used as a loading control. BLNK was highly expressed in HCT116-p21$^{-/-}$ cells after DNA damage. BLNK mRNA expression was examined by reverse transcription–polymerase chain reaction. Each expression level is shown relative to the level of BLNK at 0 h in HCT116-p53$^{+/+}$ cells. (c) Nuclear and cellular appearance of HCT116-p53$^{+/+}$, p53$^{-/-}$, and p21$^{-/-}$ cells after DNA damage. DNA damage induced micronucleate and multinucleate cells in HCT116-p53$^{-/-}$ and p21$^{-/-}$, and large polyploid cells in HCT116-p21$^{-/-}$. Images are shown 48 h after DNA damage. (d) BLNK inhibited the generation of micronucleate cells after DNA damage. HCT116-p53$^{+/+}$ or p21$^{-/-}$ cells, in which BLNK expression was downregulated with the short interfering RNA (siRNA) of BLNKsi-1 (si-1), BLNKsi-2 (si-2), and BLNKi-3 (si-3), were treated with 1.0 μg/mL adriamycin, and the numbers of mononucleate, binucleate, and micronucleate cells were counted 24 h after DNA damage. Parental HCT116-p53$^{+/+}$ and p21$^{-/-}$ cells (parent) or these cells infected with green fluorescence protein siRNA (GFPsi) were used as negative controls. Error bars ± SD (n = 4); *P < 0.01, **P < 0.001, Student's t-test between GFPsi and BLNK-si cells (si-1, si-2 and si-3). White, gray, and black bars indicate cells with mononucleate, binucleate, and multilobulated nuclei, respectively.

© 2008 Japanese Cancer Association

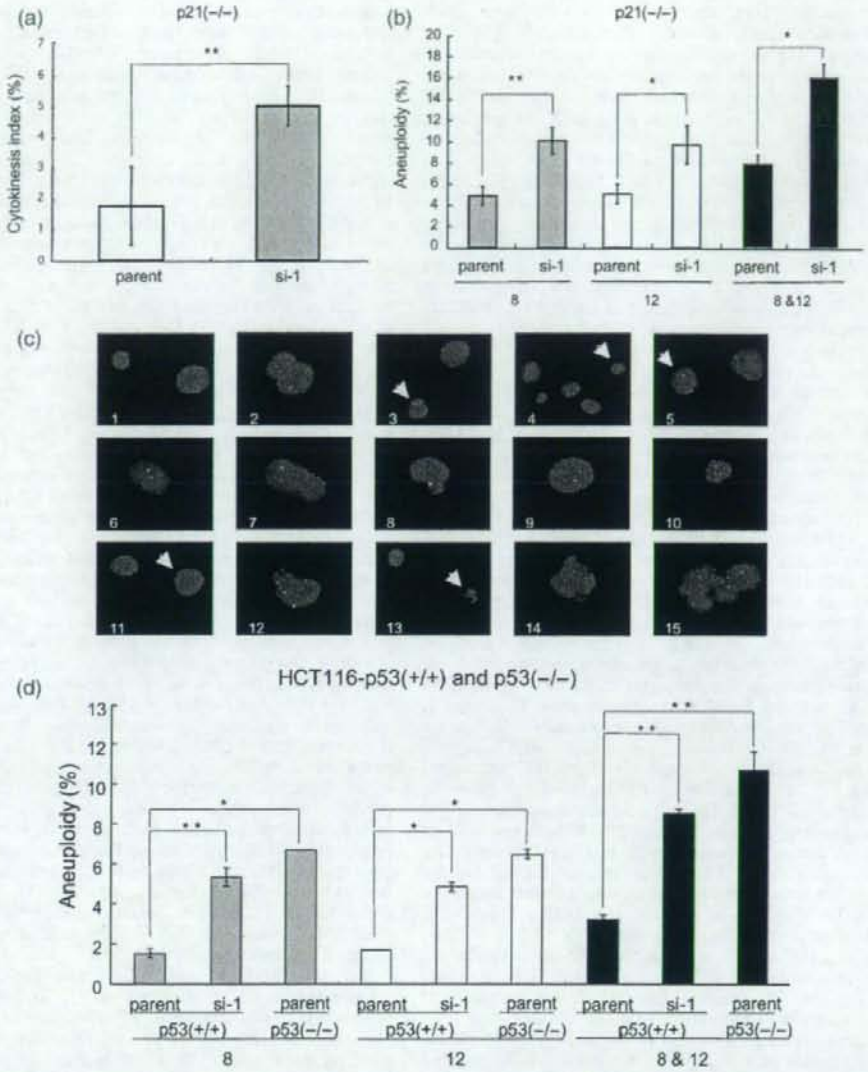

Fig. 5 B-cell linker protein (BLNK) prevents aneuploidy by inhibiting cytokinesis after DNA damage. (a) Cytokinesis enhancement by BLNK knockdown. HCT116-p21$^{-/-}$ and p21$^{-/-}$-BLNKsi-1 cells were treated with 1.0 μg/mL adriamycin, and then monitored for 24 h by time-lapse microscopy. The numbers of cells that completed cytokinesis were counted during this period. The cytokinesis index indicates the ratio of the cells that underwent cytokinesis to the total number of cells. Error bars ± SD (n = 5); $^{**}P < 0.001$, Student's t-test. (b) Impairment of BLNK induces aneuploidy after DNA damage. HCT116-p21$^{-/-}$ and p21$^{-/-}$-BLNKsi-1 cells were treated with 1.0 μg/mL adriamycin, and 24 h after treatment, the numbers of chromosomes 8 and 12 in 300 independent cells were examined by fluorescence *in situ* hybridization (FISH) analysis. Signals of 0, 1, and 3 were judged to indicate aneuploidy. The experiments were repeated four times. Error bars ± SD (n = 4); $^{*}P < 0.01$, $^{**}P < 0.001$, Student's t-test. (c) Representative results of aneuploid HCT116-p21$^{-/-}$ cells. HCT116-p21$^{-/-}$ cells were treated with 1.0 μg/mL adriamycin, and 24 h after the treatment the cells were subjected to FISH analysis, in which probes of chromosome 8 (green) and chromosome 12 (red) were used to detect aneuploidy. Signals of 0, 1, and 3 in either chromosome 8 or 9 were judged to indicate aneuploidy: 1 = diploidy (chromosome 8, 2; chromosome 12, 2); 2 = tetraploidy (chromosome 8, 4; chromosome 12, 4); 3 = aneuploidy (arrow, chromosome 8, 2; chromosome 12, 3); 4 = aneuploidy (arrow, chromosome 8, 1; chromosome 12, 2); 5 = aneuploidy (arrow, chromosome 8, 2; chromosome 12, 1); 6 = aneuploidy (chromosome 8, 1; chromosome 12, 1); 7 = aneuploidy (chromosome 8, 2; chromosome 12, 1); 8 = aneuploidy (chromosome 8, 2; chromosome 12, 0); 9 = aneuploidy (chromosome 8, 3; chromosome 12, 2); 10 = aneuploidy (chromosome 8, 3; chromosome 12, 3); 11 = aneuploidy (chromosome 8, 3; chromosome 12, 1); 12 = aneuploidy (chromosome 8, 4; chromosome 12, 3); 13 = aneuploidy (arrow, chromosome 8, 1; chromosome 12, 2); 14 = aneuploidy (chromosome 8, 3; chromosome 12, 4); 15 = aneuploidy (chromosome 8, 10; chromosome 12, 9). (d) Impairment of BLNK-induced aneuploidy after DNA damage. HCT116-p53$^{+/+}$-parent, p53$^{+/+}$-BLNKsi-1, and p53$^{-/-}$-parent cells were treated with 1.0 μg/mL adriamycin, and 24 h after the treatment the numbers of chromosomes 8 and 12 in 300 independent cells were examined by FISH analysis. Signals of 0, 1, and 3 were judged to indicate aneuploidy. Error bars ± SD (n = 2); $^{*}P < 0.05$, $^{**}P < 0.01$, Student's t-test.

doi: 10.1111/j.1349-7006.2008.00990.x
© 2008 Japanese Cancer Association

aneuploidy derived from the division of cells with DNA damage. Therefore, cytokinesis enhancement after DNA damage would cause an increase in the number of aneuploid cells. To validate this notion, we examined aneuploid cells in these lines by fluorescence *in situ* hybridization analysis with probes for chromosomes 8 and 12, as described previously.[24] Importantly, the enhancement of cytokinesis caused by the inhibition of BLNK significantly increased the number of aneuploid cells in the HCT116-p21$^{-/-}$ and HCT116-p53$^{+/+}$ cell lines (Fig. 5b,d). Representative signals of diploidy and aneuploidy are shown in Figure 5c. Interestingly, the frequency of aneuploid cells in the HCT116-p53$^{+/+}$-BLNKsi-1 cell line was similar to that in the HCT116-p53$^{-/-}$ cell line (Fig. 5d). These results strongly suggest that BLNK is involved in a p53-regulated DNA-damage checkpoint via cytokinesis inhibition, that it plays a pivotal role in the generation of mononucleate tetraploid cells in G_1 phase, and that impairment of BLNK function induces cytokinesis after DNA damage, thereby leading to aneuploidy.

Potential role of BLNK as a cytokinesis inhibitor in pre-B-cell leukemia. Finally, we evaluated the role of BLNK as a cytokinesis inhibitor in human pre-B-cell leukemia cells. BLNK was originally identified as a mediator of B-cell receptor signaling,[13–15] and its inactivation is closely related to the initiation of human and mouse pre-B-cell leukemia,[18–20] implying that it is a tumor-suppressor gene for B cells. As shown in Figure 6a, BLNK expression was severely impaired in HPB-null pre-B leukemia cells, whereas high expression levels were detected in REH and LAZ-221 pre-B leukemia cells. Interestingly, an accumulation of endogenous BLNK in the REH cell line was observed at the spindle midzone in late anaphase and at the midbody in telophase, especially overlapping the signals of Aurora-B at the midbody in late telophase (Supporting Fig. S2a). BLNK signals were also detected at the midbody in cytokinesis, and were colocalized between the two signals of Aurora-B (Supporting Fig. S2b). In addition, binucleate cells (~10%) were observed in the REH cell line, in which the BLNK signals tended to accumulate in the region between the two nuclei (Supporting Fig. 2a). Using these pre-B leukemia cell lines, we examined the status of cell division reflecting cytokinesis under various conditions, including floating or attached, and with or without DNA damage. Compared with the REH and LAZ-221 cells, the number of HPB-null cells increased more rapidly under all of the conditions tested, implying a higher frequency of cell division (Fig. 6b). In addition, the REH and LAZ-221 cells underwent cell cycle arrest with 2 N and 4 N DNA contents after DNA damage, whereas the NPB-null cells showed continued cell division and had an aneuploid DNA content (2–4 N; Fig. 6b). To validate this result, we carried out fluorescence *in situ* hybridization analysis of these cell lines with the same probes as indicated in Figure 5c. Representative signals of diploidy and aneuploidy are shown in Supporting Figure S3. As indicated in Figure 6c, we detected aneuploid cell levels of approximately 14% (chromosome 8 or 12) or 23% (both chromosome 8 and 12) after DNA damage in the HPB-null cells; these levels were approximately four times higher than those in two other cell lines expressing high levels of BLNK. Taken together, these results suggest that BLNK plays an important role in cytokinesis inhibition, in order to prevent aneuploidy after DNA damage, even in B-cell lines.

Discussion

In the present paper, we demonstrated that BLNK functions as a cytokinesis inhibitor generating tetraploidy in order to prevent aneuploidy. Based on our findings and previous reports[12,24,25] it appears likely that BLNK-induced tetraploidy plays a critical role in blocking cytokinesis of cells with chromosome miss-egregations, chromosome breakages, and DNA damage, thereby preventing the occurrence of aneuploidy. We also demonstrated that there are two major states of tetraploidy, binucleate and mononucleate, in G_1-arrested cells: the former is probably generated from spontaneous chromosome missegregations,[24] whereas the latter is likely to be a G_1-arrest DNA-damage checkpoint that is regulated by p53.[12,25] We consider the primary role of BLNK in the generation of tetraploidy to be the inhibition of cytokinesis (Figs 2,3; Supporting Fig. S2). However, the BLNK-knockdown experiment suggested that BLNK is also involved in keeping cells that have incurred DNA damage in a state of mononucleate tetraploidy at the G_1 phase of the cell cycle (Fig. 4). If this is the case, what is the regulatory mechanism for BLNK-induced mononucleate tetraploidy? Mitosis, as well as cytokinesis, did not occur during the movement of the mononucleate tetraploid cells from cell cycle phase G_2 to G_1 after DNA damage. If BLNK regulates only cytokinesis, how can the inhibition of BLNK promote mitosis? We speculate that, in addition to the inhibition of cytokinesis, BLNK might also regulate factors that trigger the start of mitosis, which determines the timing of the cell entering M phase. In fact, it is generally thought that M phase can be completed through sequential coordination of mitosis and cytokinesis, implying that the factor that regulates cytokinesis is also involved in mitosis. Further careful investigation of this process will be required to clarify the mechanism in detail.

A tetraploid-checkpoint hypothesis has been suggested to explain the p53-regulated checkpoint system.[9–12,25] In this model, p53 recognizes tetraploid cells as abnormalities, such that cell cycle is arrested at G_1 phase in a p53-dependent manner, followed by senescence or cell death. However, in our model, p53 induces tetraploidy through the activation of BLNK, in order to prevent aneuploidy. Therefore, we consider p53-induced tetraploidy, regardless of whether it is mononuleate or binucleate, to be the 'last bastion' that blocks the generation of aneuploid cells, rather than being an abnormal state (Fig. 6d). It is likely that, in response to DNA damage, p53 stops the cell cycle at G_1 phase via p21/WAF1, and blocks cytokinesis via BLNK, leading to the G_1 arrest of tetraploid cells (Fig. 6d). Consistent with previous observations,[12,25] DNA damage-induced tetraploid cells moved from cell cycle phase G_2 to G_1 without mitosis and cytokinesis in our current study. Thus, we speculate that BLNK might prevent accidental division of cells with DNA insult during their movement from cell cycle phase G_2 to G_1. We propose that p53-regulated tetraploid G_1 arrest mediated by the cooperation of p21/WAF1 and BLNK is an important safeguard system to maintain genomic integrity (Fig. 6d).

Recently, Takahashi *et al.* reported that sustained activation of reactive oxygen species–protein kinase C (ROS-PKC)σ signaling blocks cytokinesis irreversibly.[26] This irreversible cytokinetic block is likely to act as a second barrier to cellular immortalization, ensuring stable cell cycle arrest in human senescent cells.[26] Interestingly, we observed that human normal cell lines including HMEC4 and HDK1 sustained high-level BLNK protein expression at least until 7 days after DNA damage, when a senescence-like cell cycle arrest was induced in more than 50% of the cells (M. Futamura and H. Arakawa, unpublished data, 2008). Therefore, the irreversible cytokinetic block in senescent cells may be mediated by BLNK. It will be very interesting to further explore the role of BLNK in this novel tumor-suppressive mechanism.

Accumulating evidence suggests that the molecules promoting cytokinesis are strongly expressed in human cancers[27–30] and that their activation or inactivation enhances cancer cell growth or death, respectively.[27–29] Therefore, the molecules that are involved in cytokinesis progression have potential for use as molecular targets for cancer therapy.[31,32] We demonstrated that BLNK was localized at the midzone and the midbody in late anaphase, telophase, and cytokinesis (Supporting Fig. S2a), and in the middle region of the two nuclei of binucleate cells, even

© 2008 Japanese Cancer Association

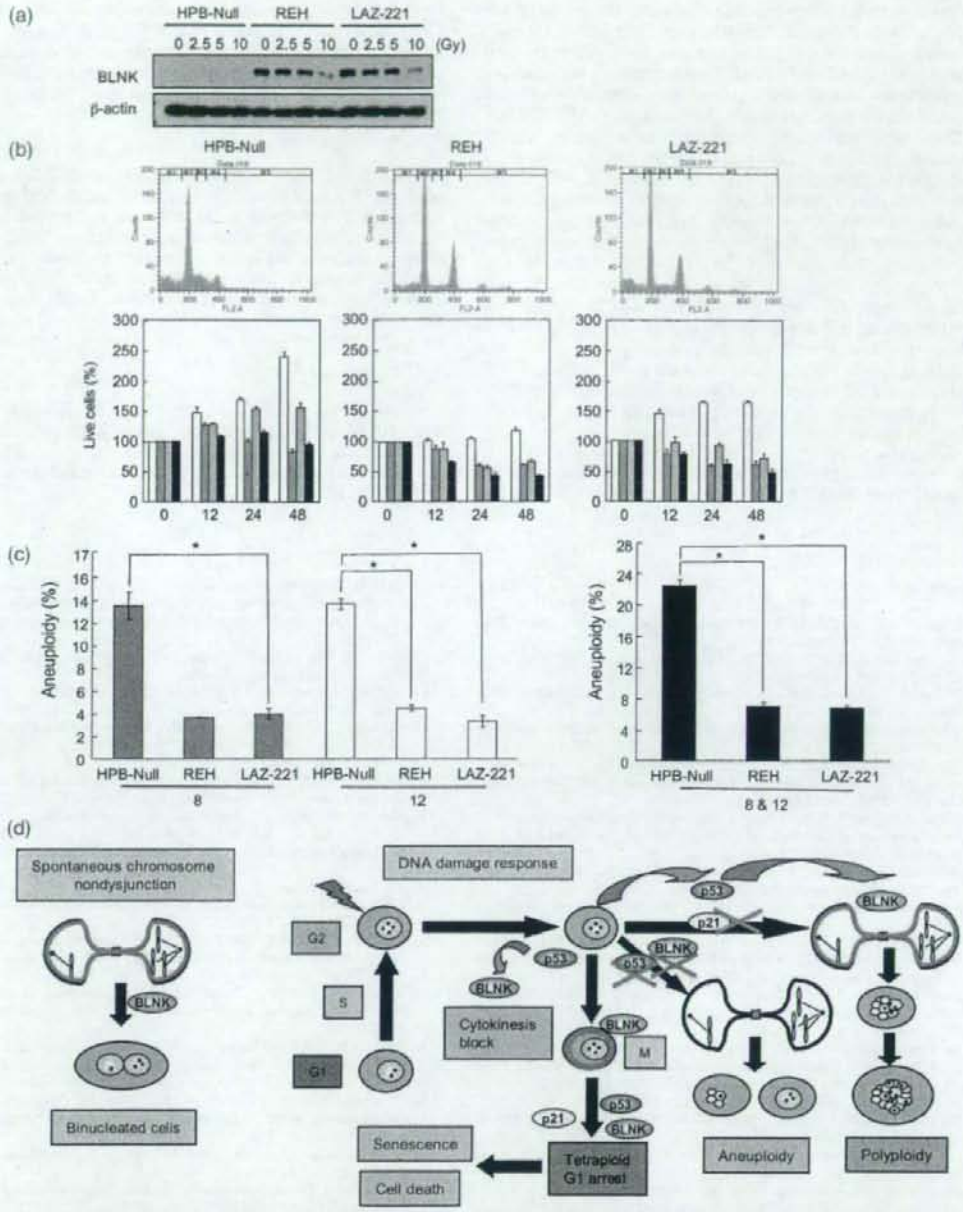

Fig. 6. Potential role of B-cell linker protein (BLNK) as an inhibitor of cytokinesis in pre-B-cell leukemia. (a) BLNK expression in human pre-B-cell leukemia. Three human pre-B-cell leukemia cell lines (HPB-null, REH, and LAZ-221) were irradiated at the indicated doses, and BLNK expression at 24 h after DNA damage was examined by western blot analysis. β-Actin was used as a loading control. (b) HPB-null cells lacking BLNK showed enhanced cell division and impaired tetraploid cell cycle arrest. Three human pre-B-cell leukemia cells (HPB-null, REH, and LAZ-221) were irradiated at 2.5 Gy, and the numbers of live cells were examined at the indicated times in the floating (gray bar) or attached (black bar) condition. The numbers of live cells without γ-irradiation were also examined at the indicated times in the floating (white bar) or attached (striped bar) condition. The DNA contents of each cell 24 h after DNA damage were determined by fluorescence activated cell sorting analysis. (c) Aneuploidy was generated preferentially from HPB-null cells lacking BLNK after DNA damage. HPB-null, REH, and LAZ-221 cells were irradiated at 2.5 Gy, and 24 h after treatment, the numbers of signals for chromosomes 8 and 12 in 300 independent cells were examined by fluorescence *in situ* hybridization analysis. Signals of 0, 1, and 3 were judged to indicate aneuploidy. The experiments were repeated twice. Error bars ± SD ($n = 2$); $^*P < 0.01$, Student's *t*-test. (d) Hypothetical model of BLNK-regulated cytokinesis.

doi: 10.1111/j.1349-7006.2008.00990.x
© 2008 Japanese Cancer Association

in interphase (Supporting Fig. S2a). In addition, the signal was colocalized with Aurora-B in cytokinesis (Supporting Fig. S2b). This result suggests a number of possible ways in which BLNK might inhibit cytokinesis. At the midzone and the midbody, Aurora-B interacts with and regulates several mediators that are involved in cytokinesis promotion, including RhoA,[33] PRC1,[34] MgcRacGAP,[35] and Plk.[36] All of these molecules are thought to promote cytokinesis, and their dysfunction causes failure of cytokinesis and multinucleate polyploidy in cells. BLNK probably interacts with at least one of these molecules to prevent cytokinesis.

On the other hand, we actually observed that the enforced expression of BLNK in U373MG cells strongly induced activation of RhoA, but not Rac1 and Cdc42 (K. Kabu and H. Arakawa, unpublished data, 2008). RhoA activation is really critical for cytokinesis progression.[21] However, at the late stage of cell division, the downregulation of RhoA activity at the midbody plays a crucial role in completion of cytokinesis probably through MgcRacGAP activation by Aurora B.[21,35] Thus, we speculate that BLNK may prevent this downregulation of RhoA activity at the midbody, resulting in the failure of cytokinesis and generation of tetraploid cells.

Although a number of cytokinesis promoters have been reported thus far, a physiological inhibitor of cytokinesis has not previously been identified. We believe that BLNK is the first candidate for a physiological cytokinesis inhibitor. Our findings thus shed light on the importance of the inhibition of cytokinesis in the maintenance of genomic integrity. In addition, our findings highlight the need for further investigations of the precise mechanism of this physiological cytokinesis inhibition.

Acknowledgments

We thank B. Vogelstein for the gift of the p53-knockout colorectal cancer cell lines, M. Kibara for the HPB-null, REH, and LAZ-221 cell lines, T. Kiyono and D.A. Galloway for the HDK1 and HMEC4 cell lines, and D. Kitamura for helpful comments on our experiments. We also thank S. Usuda, A. Ishizaka, and I. Hyo for technical assistance. This work was supported, in part, by grants from the Ministry of Health, Labour, and Welfare, Japan, and the Ministry of Education, Culture, Sports, Science, and Technology, Japan.

Author contributions

H.K., M.F., Y.N., N.K., K.K, and H.A. carried out biochemical and cell biological experiments and analyzed the data; H.K., M.F., Y.N., and H.A. designed experiments; H.K and H.A. wrote the paper. All authors discussed the results and commented on the manuscript.

References

1 Vogelstein B, Lane D, Levine AJ. Surfing the p53 network. *Nature* 2000; 408: 307–10.
2 Vousden KH. Live or let die: The cell's response to p53. *Nat Rev Cancer* 2002; 2: 594–604.
3 Nakamura Y. Isolation of p53-target genes and their functional analysis. *Cancer Sci* 2004; 95: 7–11.
4 Arakawa H. p53, apoptosis and axon-guidance molecules. *Cell Death Differ* 2005; 12: 1057–65.
5 Liu G, Parant JM, Lang G *et al.* Chromosome stability, in the absence of apoptosis, is critical for suppression of tumorigenesis in Trp53 mutant mice. *Nat Genet* 2004; 36: 63–8.
6 Barboza JA, Liu G, Ju Z, El-Naggar AK, Lozano G. p21 delays tumor onset by preservation of chromosomal stability. *Proc Natl Acad Sci USA* 2006; 103: 19 842–7.
7 Kops GJ, Weaver BA, Cleveland DW. On the road to cancer: aneuploidy and the mitotic checkpoint. *Nat Rev Cancer* 2005; 5: 773–85.
8 Rajagopalan H, Lengauer C. Aneuploidy and cancer. *Nature* 2004; 432: 338–41.
9 Margolis RL. Tetraploidy and tumor development. *Cancer Cell* 2005; 8: 353–4.
10 Margolis RL, Lohez OD, Andreassen PR. G1 tetraploidy checkpoint and the suppression of tumorigenesis. *J Cell Biochem* 2003; 88: 673–83.
11 Andreassen PR, Lohez OD, Lacroix FB, Margolis RL. Tetraploid state induces p53-dependent arrest of nontransformed mammalian cells in G1. *Mol Biol Cell* 2001; 12: 1315–28.
12 Andreassen PR, Lacroix FB, Lohez OD, Margolis RL. Neither $p21^{WAF1}$ nor 14-3-3σ prevents G2 progression to mitotic catastrophe in human colon carcinoma cells after DNA damage, but $p21^{WAF1}$ induces stable G1 arrest in resting tetraploid cells. *Cancer Res* 2001; 61: 7660–8.
13 Fu C, Turck CW, Kurosaki T, Chan AC. BLNK: a central linker protein in B cell activation. *Immunity* 1998; 9: 93–103.
14 Wienands J, Schweikert J, Wollscheid B *et al.* SLP-65: a new signaling component in B lymphocytes which requires expression of the antigen receptor for phosphorylation. *J Exp Med* 1998; 188: 791–5.
15 Goitsuka R, Fujimura Y, Mamada H *et al.* BASH, a novel signaling molecule preferentially expressed in B cells of the brusa of Fabricius. *J Immunol* 1998; 161: 5804–8.
16 Kurosaki T. Genetic analysis of B cell antigen receptor signaling. *Annu Rev Immunol* 1999; 17: 555–92.
17 Ishiai M, Kurosaki M, Pappu R *et al.* BLNK required for coupling Syk to PLC gamma 2 and Rac1-JNK in B cells. *Immunity* 1999; 10: 117–25.
18 Flemming A, Brummer T, Reth M, Jumaa H. The adaptor protein SLP-65 acts as a tumor suppressor that limits pre-B cell expansion. *Nat Immunol* 2003; 4: 13–5.
19 Jumaa H, Bossaller L, Portugal K *et al.* Deficiency of the adaptor SLP-65 in pre-B-cell acute lymphoblastic leukemia. *Nature* 2003; 423: 452–6.
20 Hayashi K, Yamamoto M, Nojima T, Goitsuka R, Kitamura D. Distinct signaling requirements for Dmu selection, IgH allelic exclusion, pre-B cell transition, and tumor suppression in B cell progenitors. *Immunity* 2003; 18: 825–36.
21 Piekny A, Werner M, Glotzer M. Cytokinesis: welcome to the Rho zone. *Trends Cell Biol* 2005; 15: 651–8.
22 Straight AF, Field CM. Microtubules, membrane and cytokinesis. *Curr Biol* 2000; 10: R760–70.
23 Masuda Y, Futamura M, Kamino H *et al.* The potential role of DFNA5, a hearing impairment gene, in p53-mediated cellular response to DNA damage. *J Hum Genet* 2006; 51: 652–64.
24 Shi Q, King RW. Chromosome nondisjunction yields tetraploid rather than aneuploid cells in human cell lines. *Nature* 2005; 437: 1038–42.
25 Bhonde MR, Hanski ML, Notter M *et al.* Equivalent effect of DNA damage-induced apoptotic cell death or long-term cell cycle arrest on colon carcinoma cell proliferation and tumour growth. *Oncogene* 2006; 25: 165–75.
26 Takahashi A, Ohtani N, Yamakoshi K *et al.* Mitogenic signalling and the p16INF4a-Rb pathway cooperate to enforce irreversible cellular senescence. *Nat Cell Biol* 2006; 8: 1291–7.
27 Shimo A, Nishidate T, Ohta T *et al.* Elevated expression of protein regulator of cytokinesis 1, involved in the growth of breast cancer cells. *Cancer Sci* 2007; 98: 174–81.
28 Kanehira M, Katagiri T, Shimo A *et al.* Oncogenic role of MPHOSPH1, a candidate-testis antigen specific to human bladder cancer. *Cancer Res* 2007; 67: 3276–85.
29. Hayama S, Daigo Y, Yamabuki T *et al.* Phosphorylation and activation of cell division associated 8 by aurora kinase B plays a significant role in human lung carcinogenesis. *Cancer Res* 2007; 67: 4113–22.
30 Vishioni B, Oudejans JJ, Vos W, Rodriguez JA, Giaccone G. Frequent overexpression of aurora B kinase, a novel drug target, in non-small lung carcinoma patients. *Mol Cancer Ther* 2006; 5: 2905–13.
31 Keen N, Taylor S. Aurora-kinase inhibitors as anticancer agents. *Nat Rev Cancer* 2004; 4: 927–36.
32 Carvajal RD, Tse A, Schwartz GK. Aurora kinases: new targets for cancer therapy. *Clin Cancer Res* 2006; 12: 6869–75.
33 Yoshizaki H, Ohba Y, Kurokawa K *et al.* Activity of Rho-family GTPase during cell division as visualized with FRET-based probes. *J Cell Biol* 2003; 162: 223–32.
34 Jiang W, Jimenez G, Wells NJ *et al.* PRC1: a human mitotic spindle-associated CDK substrate protein required for cytokinesis. *Mol Cell* 1998; 2: 877–85.
35 Minoshima Y, Kawashima T, Hirose K *et al.* Phosphorylation by Aurora B converts MgcRacGAP to a RhoGAP during cytokinesis. *Dev Cell* 2003; 4: 549–60.
36 Nigg EA. Polo-like kinases: positive regulators of cell division from start to finish. *Curr Opin Cell Biol* 1998; 10: 776–83.

© 2008 Japanese Cancer Association

Supporting information

Additional Supporting Information may be found in the online version of this article:

Fig. S1. Inhibition of B-cell linker protein (BLNK) expression by short interfering RNA in HCT116-p53$^{+/+}$ and HCT116-p21$^{-/-}$ cells. (a) Downregulation of BLNK mRNA expression in (a) HCT116-p53$^{+/+}$ and (b) HCT116-p21$^{-/-}$ cells. Various cells, including parental (P), GFPsi (G), BLNKsi-1 (si-1), BLNKsi-2 (si-2), and BLNKsi-3 (si-3), were treated with 1.0 μg/mL adriamycin, and the BLNK mRNA expression levels were examined by real-time polymerase chain reaction 24 and 48 h after DNA damage. The expression levels are shown relative to the level (= 1) of (a) HCT116-p53$^{+/+}$ and (b) HCT116-p21$^{-/-}$ parental cells without DNA damage.

Fig. S2. Localization of B-cell linker protein (BLNK) at the mid-zone and mid-body during late anaphase, telophase, and cytokinesis. BLNK and Aurora B were colocalized at the mid-body in telophase. In REH cells, BLNK (green) and Aurora B (red) proteins were stained with anti-BLNK and anti-Aurora B antibodies, respectively. DNA (blue) was stained with Topro 3.B, BLNK and Aurora B were localized at the midbody in cytokinesis. BLNK (green) was localized at the center of the midbody between the two signals (red) of Aurora B in cytokinesis.

Fig. S3. Aneuploidy was preferentially generated from HPB-null cells lacking B-cell linker protein (BLNK) after DNA damage. Representative fluorescence *in situ* hybridization images are shown. The signals indicate the number of chromosomes 8 (green) and 12 (red): 1 = diploidy (chromosome 8, 2; chromosome 12, 2); 2 = aneuploidy (chromosome 8, 1; chromosome 12, 1); 3 = aneuploidy (chromosome 8, 2; chromosome 12, 0); 4 = aneuploidy (chromosome 8, 1; chromosome 12, 2); 5 = aneuploidy (chromosome 8, 2; chromosome 12, 1); 6 = aneuploidy (arrow, chromosome 8, 3; chromosome 12, 2). The individual (8 or 12) and combined (8 and 12) are shown.

Please note: Wiley-Blackwell are not responsible for the content or functionality of any supporting materials supplied by the authors. Any queries (other than missing material) should be directed to the corresponding author for the article.

doi: 10.1111/j.1349-7006.2008.00990.x
© 2008 Japanese Cancer Association

Suppression of hPOT1 in Diploid Human Cells Results in an hTERT-Dependent Alteration of Telomere Length Dynamics

Richard Possemato,[1] Jamie C. Timmons,[1] Erica L. Bauerlein,[1] Naoya Wada,[1] Amy Baldwin,[2] Kenkichi Masutomi,[4] and William C. Hahn[1,3]

[1]Department of Medical Oncology, Dana-Farber Cancer Institute and Department of Medicine, Brigham and Women's Hospital and Harvard Medical School; [2]The Channing Laboratory, Brigham and Women's Hospital and Department of Medicine, Harvard Medical School, Boston, Massachusetts; [3]Broad Institute of Harvard and Massachusetts Institute of Technology, Cambridge, Massachusetts; and [4]National Cancer Center, Cancer Stem Cell Project, Tokyo, Japan

Abstract

POT1 is a 3′ telomeric single-stranded overhang binding protein that has been implicated in chromosome end protection, the regulation of telomerase function, and defining the 5′ chromosome terminus. In human cancer cells that exhibit constitutive hTERT activity, hPOT1 exerts control over telomere length. Primary human fibroblasts express low levels of catalytically active hTERT in an S-phase–restricted manner that fails to counteract telomere attrition with cell division. Here, we show that diploid human fibroblasts in which *hPOT1* expression has been suppressed harbor telomeres that are longer than control cells. This difference in telomere length delays the onset of replicative senescence and is dependent on S-phase–restricted hTERT expression. These findings are consistent with the view that hPOT1 promotes a nonextendable telomere state resistant to extension by S-phase–restricted telomerase. Manipulating this function of hPOT1 may thus hasten the cytotoxic effects of telomerase inhibition. (Mol Cancer Res 2008;6(10):1582–93)

Introduction

Telomeres are nucleoprotein complexes that cap the termini of eukaryotic chromosomes (1). Mammalian telomeres contain several thousand base pairs of TTAGGG repeats and end in a several hundred base pair 3′ extension of the G-rich strand that is required for the formation of a t-loop structure (2). Telomerase is a ribonucleoprotein reverse transcriptase composed of a catalytic protein subunit, TERT, and a RNA subunit, *TERC*, which together synthesize additional telomeric repeats (3-5). Dyskerin, a RNA-binding molecule that participates in ribonucleoprotein assembly, is associated with catalytically active telomerase (6) and several other proteins have been reported to be associated with telomerase (7). In normal human cells, telomerase activity is tightly regulated. Although *TERC* is expressed constitutively in most cells, hTERT expression is restricted to low levels in S phase of the cell cycle in most diploid nonmalignant cells (8). This low-level hTERT expression fails to maintain telomere length in such cells, and approximately 30 to 100 bp of telomeric DNA are lost per cell division (9). However, it is unclear whether this inability to maintain telomere length is because this low level of hTERT is not competent to act on telomeres or because of a suppressive mechanism inhibiting telomerase action at telomeres in these cells.

Normal human cells reach a replicative limit characterized by entrance into a growth-arrested state termed replicative senescence, which can be triggered in part by dysfunctional telomeres (10). In these cells, entry into replicative senescence requires intact p53 or pRB cell cycle checkpoints (11, 12). In contrast, most immortalized and transformed cells exhibit constitutively high levels of telomerase activity, which correlates with stable telomere length (3, 13). This observation suggests that telomerase activation in premalignant cells results in an immortalized state that is required for tumorigenesis. In support of this hypothesis, overexpression of hTERT facilitates cell immortalization (14), whereas inhibition of telomerase either genetically or pharmacologically in already immortal cancer cell lines results in loss of telomeric sequences, a loss of proliferative capacity, and the onset of crisis (15-17). Consistent with the view that telomerase activation plays an important role in facilitating human cell transformation, coexpression of hTERT with cooperating oncogenes, such as the SV40 large T and small T antigens and RAS, generates tumorigenic cells (18).

Telomere homeostasis is regulated by a multiprotein complex known as the telosome/shelterin complex (19). The results from studies focused on the control of telomere length by telomere-binding proteins suggest that such proteins make up a binary switch that controls whether a telomere is in an extendible or nonextendible state (20). In their initial studies

Received 2/6/08; revised 5/16/08; accepted 6/19/08.
Grant support: NIH National Institute on Aging grant R01 AG23145 and Johnson and Johnson Focused Giving Program Award. R. Possemato was supported by a Howard Hughes Predoctoral Fellowship.
The costs of publication of this article were defrayed in part by the payment of page charges. This article must therefore be hereby marked *advertisement* in accordance with 18 U.S.C. Section 1734 solely to indicate this fact.
Note: Supplementary data for this article are available at Molecular Cancer Research Online (http://mcr.aacrjournals.org/).
Requests for reprints: William C. Hahn, Dana-Farber Cancer Institute, 44 Binney Street, Boston, MA 02115. Phone: 617-632-2641; Fax: 617-632-4005. E-mail: william_hahn@dfci.harvard.edu
Copyright © 2008 American Association for Cancer Research.
doi:10.1158/1541-7786.MCR-08-0070

in *Schizosaccharomyces pombe*, Baumann and Cech (21) identified POT1 as a novel telomere-binding protein and a component necessary for the maintenance of a stable telomere. Subsequent genetic and biochemical studies have identified a role for POT1 in telomere length maintenance and telomere capping (22). Overexpression of full-length or alternatively spliced hPOT1 (23) or suppression of *hPOT1* by short hairpin RNA (shRNA; refs. 24, 25) in the telomerase-positive cell line HT1080 led to telomere elongation, whereas overexpression of mutant forms of hPOT1 lacking the 5′ oligonucleotide-binding fold domains led to telomere elongation in HTC75/HT1080 cells (22, 26). Recently, a POT1-interacting protein, TPP1, has been identified, which regulates localization of POT1 to the telomere (25, 26) and mediates telomere length control in concert with POT1 (27-29).

In primer extension assays, the ability of POT1 to regulate telomere addition to artificial substrates depended on primer composition. Primers that can fold into telomerase inaccessible G-quadruplex structures were resolved by the addition of POT1 and led to an increase in extension from these primers (30). Alternatively, extension from shorter primers was inhibited by POT1 (31, 32), but elongation, when it occurred, did so with increased processivity (32).

Unlike humans, two very similar POT1 genes, *POT1a* and *POT1b*, are present in mice (33). Two groups have reported that targeted deletion of *POT1a* results in embryonic lethality in the mouse; however, these groups found both telomere elongation (34) and no change in overall telomere length (35) after germline deletion of *POT1a*. In contrast, targeted deletion of *POT1b* fails to change overall telomere length but results in *mTERC*-independent 3′ overhang lengthening (35).

Despite these extensive studies into the biology of POT1, the role of hPOT1 in regulating telomerase and telomere length in primary human cells or in cells lacking hTERT is currently unknown. Here, we explored the consequences of suppressing *hPOT1* under conditions where *hTERT* was constitutively expressed, S-phase restricted, or suppressed. We found that suppression of *hPOT1* alters the dynamics of telomere length control in an hTERT-dependent manner. These observations have implications for the timing of the entry of these cells into replicative senescence.

Results

Telomere Length Dynamics of Primary Human Fibroblasts

To understand the role of hPOT1 in telomere length control in primary human cells, we generated lentiviral vectors coexpressing a puromycin or neomycin selectable marker and a shRNA that targets all known *hPOT1* splice variants (hPOT1sh #1 puro and hPOT1sh #1 neo) or a shRNA that targets an unrelated sequence (CONsh puro or CONsh neo) and introduced these shRNAs into mortal BJ human fibroblasts. Expression of either hPOTsh #1 puro or hPOT1sh #1 neo induced a 75% decrease in the expression of hPOT1 as assessed by quantitative reverse transcription-PCR (RT-PCR) or immunoblotting (Fig. 1A).

To determine if suppressing hPOT1 expression and overexpressing hTERT in diploid fibroblasts resulted in an increased rate of telomere lengthening, we then infected BJ cells expressing CONsh neo or hPOT1sh #1 neo with a retrovirus encoding the *hTERT* cDNA (BJ CONsh+ hTERT and BJ hPOT1sh #1+ hTERT). Genomic DNA was isolated from these four cell lines (BJ CONsh, BJ hPOT1sh #1, BJ CONsh+ hTERT, and BJ hPOT1sh #1+ hTERT) every two population doublings (PDs) following infection and analyzed by telomere restriction fragment (TRF) Southern blotting to determine mean TRF length. In consonance with prior reports (9, 14), the mean telomere length decreased by 41 bp/PD in BJ CONsh cells, whereas BJ CONsh+ hTERT cells exhibited overall telomere lengthening of 101 bp/PD (Fig. 1B and C, *odd lanes*). We noted a uniform decrease in TRF length in the BJ CONsh cell population, characterized by an increase in the signal of shorter fragments (compare Fig. 1B, *lanes 1* and *11* and see Fig. 1D, *top left*). When hTERT was expressed constitutively at high levels, we observed that the shortest TRFs increased in size rather than a uniform lengthening of telomeres of all lengths (compare Fig. 1C, *lanes 1* and *11* and see Fig. 1D, *bottom left*) as has been described in murine cells (36).

Surprisingly, we observed an altered telomere shortening dynamic in BJ cells in which *hPOT1* had been suppressed. Over the time course of this experiment, we detected relatively little change in the abundance of shorter TRFs (compare Fig. 1B, *lanes 2* and *12* and see Fig. 1D, *top middle*). Consequently, when compared with control cells, the rate of telomere shortening in BJ hPOT1sh #1 cells was reduced by 52% to 20 bp/PD (Fig. 1B). After 12 PDs, this difference in the rate of telomere attrition results in a 400-bp increase in mean TRF length between BJ hPOT1sh #1 and BJ CONsh cells (compare Fig. 1B, *lanes 11* and *12* and see Fig. 1D, *top right*). Specifically, BJ CONsh cells exhibited stronger signals for TRF fragments shorter than 7 kb (Fig. 1D, *top right*).

We found that either suppressing *hPOT1* or overexpressing hTERT resulted in a smaller proportion of shorter TRF fragments with a corresponding greater proportion of longer fragments (compare Fig. 1C, *lanes 1* and *11* for BJ CONsh+ hTERT cells and Fig. 1B, *lanes 11* and *12* for BJ hPOT1sh #1 cells and see Fig. 1D, *bottom left* and *top right*). Cells in which both *hTERT* was overexpressed and *hPOT1* was suppressed exhibited a 400-bp difference in telomere length within two PDs after introduction of *hTERT* compared with cells overexpressing *hTERT* alone (compare Fig. 1C, *lanes 1* and *2* and see Fig. 1D, *bottom middle*). Subsequent telomere elongation proceeded at the same rate in both populations, and thus, BJ hPOT1sh #1+ hTERT cells maintained an increased telomere length throughout the course of this experiment (compare Fig. 1C, *lanes 1* and *2* with *lanes 11* and *12* and see Fig. 1D, *bottom middle* and *bottom right*). Taken together, these observations suggest that constitutive expression of *hTERT* and suppression of *hPOT1* likely affect telomere length and/or structure in different ways.

To address the possibility that the observed telomere elongation phenotype was due to an off-target effect of RNA interference, we generated a full-length hPOT1 cDNA that is resistant to hPOT1sh #1 by introducing five nucleotide substitutions that do not change the amino acid coding sequence (hPOT1R). We introduced hPOT1R or a control vector into BJ and BJ hTERT cells (BJ hPOT1R and BJ hTERT hPOT1R). Expression of hPOT1R resulted in hPOT1 overexpression, which persisted after subsequent introduction of hPOT1sh #1, whereas the control vector permitted *hPOT1* suppression after

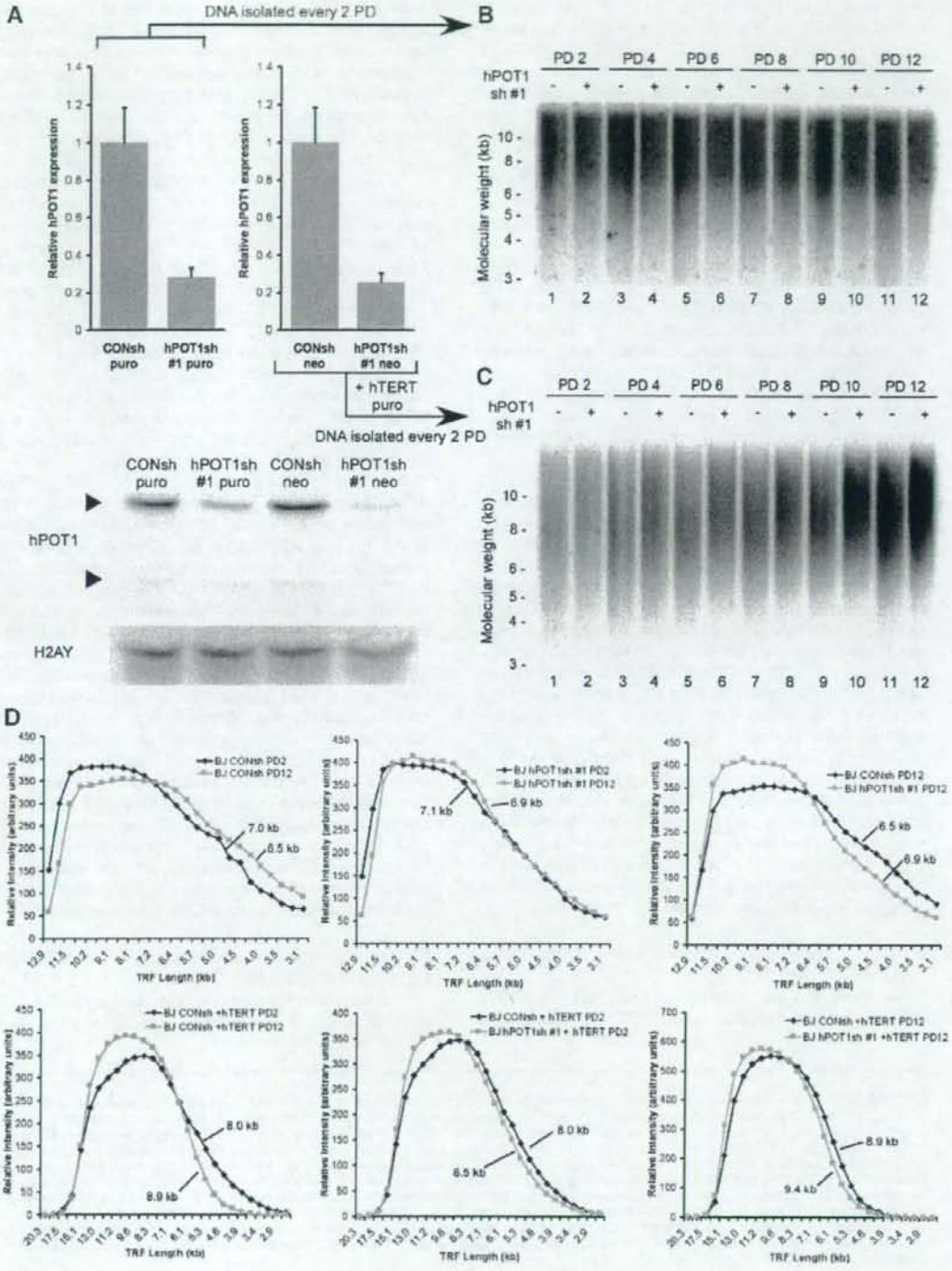
A
DNA isolated every 2 PD
Relative hPOT1 expression
CONsh puro
hPOT1sh #1 puro
CONsh neo
hPOT1sh #1 neo
+ hTERT puro
DNA isolated every 2 PD
CONsh puro
hPOT1sh #1 puro
CONsh neo
hPOT1sh #1 neo
hPOT1
H2AY
B
PD 2
PD 4
PD 6
PD 8
PD 10
PD 12
hPOT1 sh #1
Molecular weight (kb)
C
D
TRF Length (kb)
7.0 kb
8.5 kb
7.1 kb
6.9 kb
6.5 kb
8.0 kb
8.9 kb
9.4 kb

introduction of hPOT1sh #1 (Fig. 2A). In BJ cells containing a control vector, we again found a statistically significantly increase ($P \leq 0.000009$) in TRF length of 230 bp on introduction of hPOT1sh #1 (Fig. 2B). In contrast, in BJ hPOT1R cells, we failed to observe telomere elongation on introduction of hPOT1sh #1 (Fig. 2B), suggesting that the telomere elongation phenotype was not the result of off-target effects of RNA interference.

To determine if suppressing hPOT1 expression in diploid human fibroblasts that overexpress hTERT induced increased telomere length as has been observed in other telomerase-positive human cell lines (24, 25), we suppressed *hPOT1* in BJ hTERT cells and also observed a statistically significant increase ($P \leq 0.000032$) in telomere length that was abolished in cells coexpressing hPOT1R (Fig. 2B and C). The BJ hTERT fibroblasts used in these experiments had been passaged until they had achieved a stable maximum telomere length, allowing us to measure the effects of *hPOT1* suppression on this maximal telomere length set point. Suppression of *hPOT1* in the hTERT-immortalized BJ cells resulted in telomere elongation of ~340 bp beyond the stable maximum length as assessed by TRF Southern blotting (Fig. 2B).

Although the observed differences in telomere length are statistically significant, the differences in telomere length being detected in these experiments are at the limit of sensitivity for TRF Southern blotting. Moreover, the estimation of size of the longest telomere lengths is less precise than that of shorter lengths. To confirm these measurements using a second approach, we used quantitative fluorescence *in situ* hybridization (FISH). This method does not measure subtelomeric repeats, which comprise a much greater fraction of the TRF signal in primary cells (37), and therefore, differences in telomere lengths as a percentage of overall telomere length are expected to be larger using this technique. As expected, when comparing primary BJ cells expressing CONsh with those expressing hPOT1sh #1, we noted an increase in fluorescence of 29%, which was abolished in cells expressing hPOT1R (Fig. 2C). Similarly, when comparing BJ hTERT cells with those expressing hPOT1sh #1, we noted an increase in fluorescence of 5.8%, which was also abolished by expression of hPOT1R (Fig. 2C). Together, these observations show that suppressing *hPOT1* in both mortal and immortal human fibroblasts leads to telomere elongation and telomere maintenance at a new set point.

Effects of Replicative History on the Response of Fibroblasts to hPOT1 Suppression

We found that the introduction of two different *hPOT1* shRNAs into early-passage BJ and BJ hTERT cells increased the short-term doubling time of the cells by 10% to 20% (Fig. 3A). A previous report showed that suppression of *hPOT1* had no effect on the doubling time of immortal fibroblasts but increased the short-term doubling time of nonimmortal human fibroblasts by approximately 30% to 40% (38). In contrast, others have shown more dramatic effects of *hPOT1* suppression on proliferative rates (24, 39). We speculated that the replicative history of the cells dictated their response to suppression of *hPOT1*.

To test this hypothesis, we obtained freshly isolated human foreskin fibroblasts (HFF) or used the aforementioned BJ fibroblasts. After allowing the cultures to proliferate for 0 to 40 additional PDs, we introduced one of two shRNAs targeting all known splice variants of *hPOT1* (hPOT1sh #1 or hPOT1sh #2) or a control sequence (CONsh). *hPOT1* was suppressed to similar levels in each of these cell populations, although we noted diminished hPOT1 expression in HFF cells that had undergone 40 PDs or BJ cells that had undergone 54 PDs (Fig. 3B). Suppression of *hPOT1* in the HFF and BJ cells that had proliferated for the longest time in culture resulted in a 2- to 4-fold greater increase in doubling time as well as a marked induction in senescence-associated β-galactosidase (SA β-gal) staining (Fig. 3A and C; Supplementary Fig. S1).

Prior work has shown that suppression of *hPOT1* resulted in the appearance of telomere dysfunction–induced foci (TIF; ref. 38). To determine whether TIFs were present in cells in which *hPOT1* has been suppressed, we costained the early- and late-passage BJ cells described above for S15 phosphorylated histone H2AX (γ-H2AX) as a marker of DNA damage and a labeled PNA telomeric probe. We found colocalization of γ-H2AX and telomeric foci in both early- and late-passage cells in which *hPOT1* was suppressed (Fig. 3D and E). Although we observed γ-H2AX staining in control and *hPOT1*-suppressed cells, little to no colocalization with telomeres was detected in cells expressing the control shRNA (Fig. 3D and E). The percentage of cells exhibiting γ-H2AX and telomeric focus colocalization was similar in early- and late-passage BJ cells. However, we also observed DNA bridges in late-passage cells that lack *hPOT1* expression at a frequency of 4% (8 of 200 nuclei; Fig. 3F). Taken together, these observations suggest that suppression of *hPOT1* results in telomere dysfunction in all cells regardless of passaging history. However, early-passage cells are able to tolerate this damage, whereas in later-passage cells suppression of *hPOT1* results in telomere uncapping and the onset of senescence.

Long-term Effects of Suppressing hPOT1 on Telomere Length and Proliferative Life Span

With successive cell divisions, mortal human fibroblasts lose telomere length at the rate of approximately 30 to 50 bp/PD (9).

FIGURE 1. Effects of suppressing hPOT1 on telomere dynamics. **A.** hPOT1 mRNA and protein levels. mRNA levels were determined by quantitative RT-PCR (*top*) and hPOT1 protein levels by immunoblotting (*bottom*) in BJ cells expressing either an hPOT1 shRNA (*hPOT1sh #1*) or a control shRNA (*CONsh*) in lentiviral constructs containing either puromycin (*puro*) or neomycin (*neo*) selection markers. Columns, mean of triplicate experiments; bars, SD. Arrows, hPOT1 isoforms. **B.** TRF Southern blotting of mortal BJ cells with passage. DNA was collected at the indicated PDs after infection with CONsh (−) or hPOT1sh #1 (+). Left, DNA size markers in kb. **C.** TRF Southern blotting of BJ cells that overexpress hTERT with successive passage. DNA was collected at the indicated PD after infection with a retrovirus encoding the hTERT cDNA in cells previously infected with CONsh (−) or hPOT1sh #1 (+). Lanes are numbered 1 to 12 for reference. **D.** Densitometry of selected lanes. The relative intensity at regular TRF length intervals is shown and mean TRF lengths for the entire lane are indicated. Top left, compares **B**, lanes 1 (*black diamonds*) and 11 (*gray squares*); top middle, compares **B**, lanes 2 (*black diamonds*) and 12 (*gray squares*); top right, compares **B**, lanes 11 (*black diamonds*) and 12 (*gray squares*); bottom left, compares **C**, lanes 1 (*black diamonds*) and 11 (*gray squares*); bottom middle, compares **C**, lanes 1 (*black diamonds*) and 2 (*gray squares*); bottom right, compares **C**, lanes 11 (*black diamonds*) and 12 (*gray squares*).

Because cells in which *hPOT1* was suppressed exhibited diminished telomere shortening, we assessed the effects of suppressing *hPOT1* on telomere lengths over extended passage and on replicative life span. We cultured HFF and BJ cells expressing CONsh or hPOT1sh #1 or hPOT1sh #2 and determined telomere length as a function of PD. Although cells in which *hPOT1* was suppressed exhibited a longer mean telomere length over time relative to control cells, both populations eventually showed a reduction in mean telomere length at a similar rate (Fig. 4A and B). This observation contrasts with the decrease in telomere shortening rate seen immediately after suppression of *hPOT1*, suggesting that cells in which *hPOT1* has been suppressed reach a new stable telomere length set point after which normal telomere attrition occurs.

To assess the effects of *hPOT1* suppression in human fibroblasts on replicative senescence, we assessed the long-term proliferative capacity of BJ or BJ hTERT fibroblasts expressing CONsh or hPOT1sh #1 or hPOT1sh #2. Suppression of *hPOT1* in immortal BJ fibroblasts did not affect proliferative capacity over the course of 100 days (Fig. 4C). However, suppression of *hPOT1* in mortal BJ fibroblasts led to a statistically significant extension of the number of PD required to reach senescence (10 PDs; Fig. 4D). This increase in proliferative capacity correlated with the predicted additional PD possible due to the additional telomere length found in cells in which *hPOT1* was

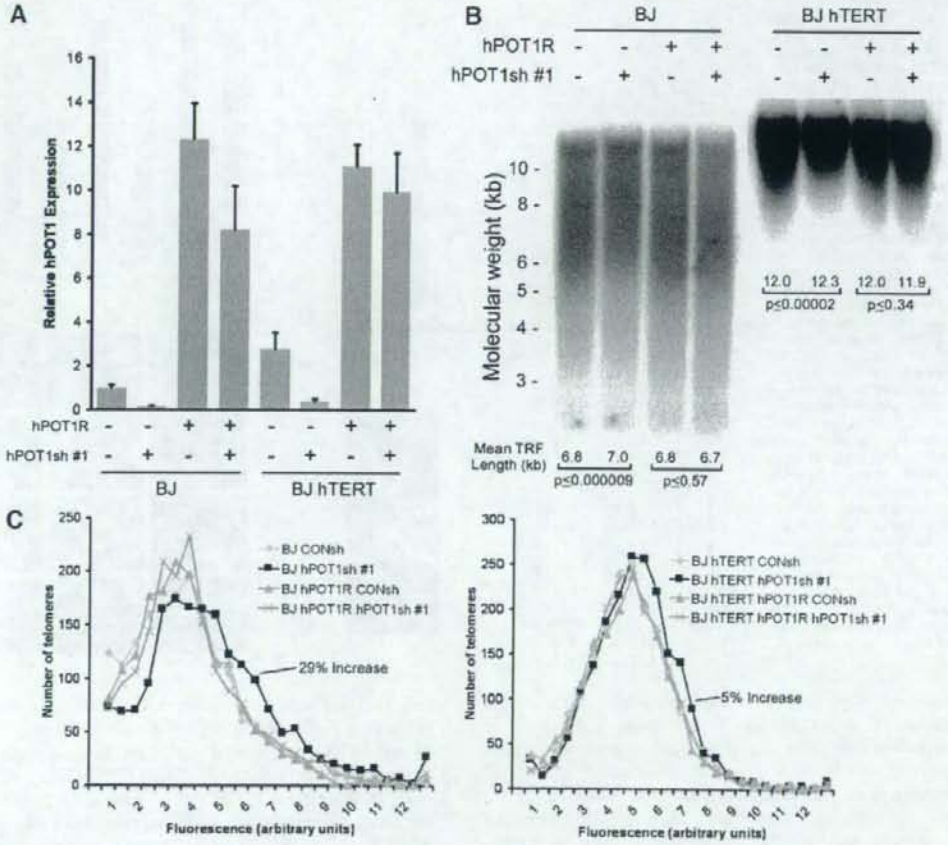

FIGURE 2. Rescue of telomere length changes induced by *hPOT1* suppression. **A.** Overexpression of *hPOT1*. hPOT1 mRNA levels in BJ or BJ hTERT cells expressing a control hairpin (CONsh) or an hPOT1 hairpin (hPOT1sh #1) in cells expressing the hPOT1sh #1–resistant version of hPOT1 (*hPOT1R*). **B.** TRF Southern blotting showing rescue of *hPOT1* suppression. The mean TRF length for each sample taken 10 PDs after infection is indicated beneath the corresponding lane. *P* values (two-tailed *t* test) are shown for the indicated pairwise comparisons from three (BJ) or four (BJ hTERT) replicate experiments. DNA size markers in kb shown on the left are for both gels. **C.** Quantitative telomere FISH showing rescue of *hPOT1* suppression. Results are shown for 12 metaphases for the BJ (*left*) and BJ hTERT (*right*) cell lines characterized in **A** and **B**. The fluorescence intensity of telomeres from each sample was assigned into a bin, the intensity of which is indicated on the *X* axis and the number of telomeres contained within that bin is indicated on the *Y* axis. The percent increase in mean fluorescence intensity for the hPOT1sh #1 versus CONsh cell line is indicated. Fluorescence values are arbitrary and cannot be compared between graphs.

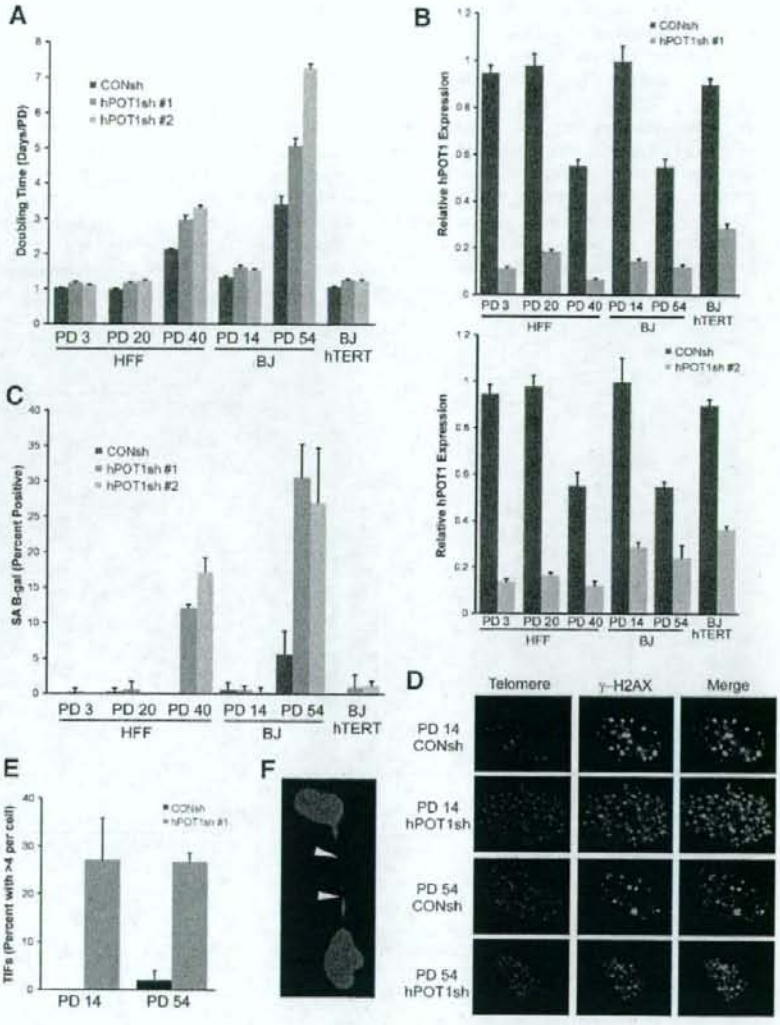

FIGURE 3. Short-term effects of *hPOT1* suppression in cells of different proliferative age. **A.** Doubling times of BJ and HFF cells. BJ or HFF cells infected with a control hairpin (*CONsh*) or one of two hairpins targeting *hPOT1* (*hPOT1sh #1* or *hPOT1sh #2*) at the cumulative PD indicated. Doubling times were measured over 13 to 17 d in triplicate. **B.** *hPOT1* mRNA levels in BJ and HFF cells at the indicated PD. Expression of hPOT1 for cell lines characterized in **A** using primers near the hPOT1sh #1 (*top*) or hPOT1sh #2 (*bottom*) targeting site. **C.** SA β-gal staining. Values represent the percentage of cells that stained for SA β-gal. For these experiments, at least 100 total cells were scored in triplicate. **D.** TIF images. Staining for γ-H2AX (*green*) and telomeric DNA (*red*) are shown from two cells expressing hPOT1sh #1 that exhibited significant TIF formation and two cells expressing CONsh that exhibited little to no TIF formation. **E.** Quantification of TIF formation. Values represent the percentage of nuclei containing more than four foci costaining for γ-H2AX by indirect immunofluorescence and telomeric DNA by PNA FISH. At least 100 nuclei were scored in three independent experiments. **F.** DNA bridge formation. 4′,6-Diamidino-2-phenylindole–stained image of a representative DNA bridge (*arrows*) between two nuclei from PD 54 cells expressing hPOT1sh #1. DNA bridges were identified in 4% (8 of 200) of nuclei scored.

suppressed. Consistent with this observation, control cells exhibited a 2-fold increase in SA β-gal staining at an intermediate time point (Fig. 4E). Together, these observations indicated that there is a dichotomous effect of *hPOT1* suppression on human fibroblasts: acute induction of the senescent state in later-passage cells and tolerance and extension in the time to replicative senescence in earlier-passage cells.

Dependence of the Telomere Length Effects of hPOT1 Suppression on hTERT Expression

To determine whether the telomere length phenotype seen in *hPOT1*-suppressed cells is dependent on the presence of S-phase–restricted hTERT, we generated a series of BJ and HFF cell lines in which we suppressed *hTERT* expression by introducing two different *hTERT*-specific shRNAs (hTERTsh #1 and hTERTsh #2). In BJ cells, we also overexpressed a catalytically inactive mutant of hTERT (DN-hTERT), which we had previously shown to inhibit telomerase activity (15). We confirmed suppression of *hTERT* expression in these cells by RT-PCR and expression of DN-hTERT by immunoblotting (Fig. 5A). We note that suppression of *hTERT* led to an increase in hPOT1 expression in BJ but not in HFF cells (Fig. 5B). Despite this change in hPOT1 levels, expression of hPOT1sh #1 in these cell lines was able to suppress *hPOT1* to similar levels (Fig. 5B).

Analysis of telomere length in both BJ and HFF cells showed that suppression of *hTERT* by shRNA or inhibition

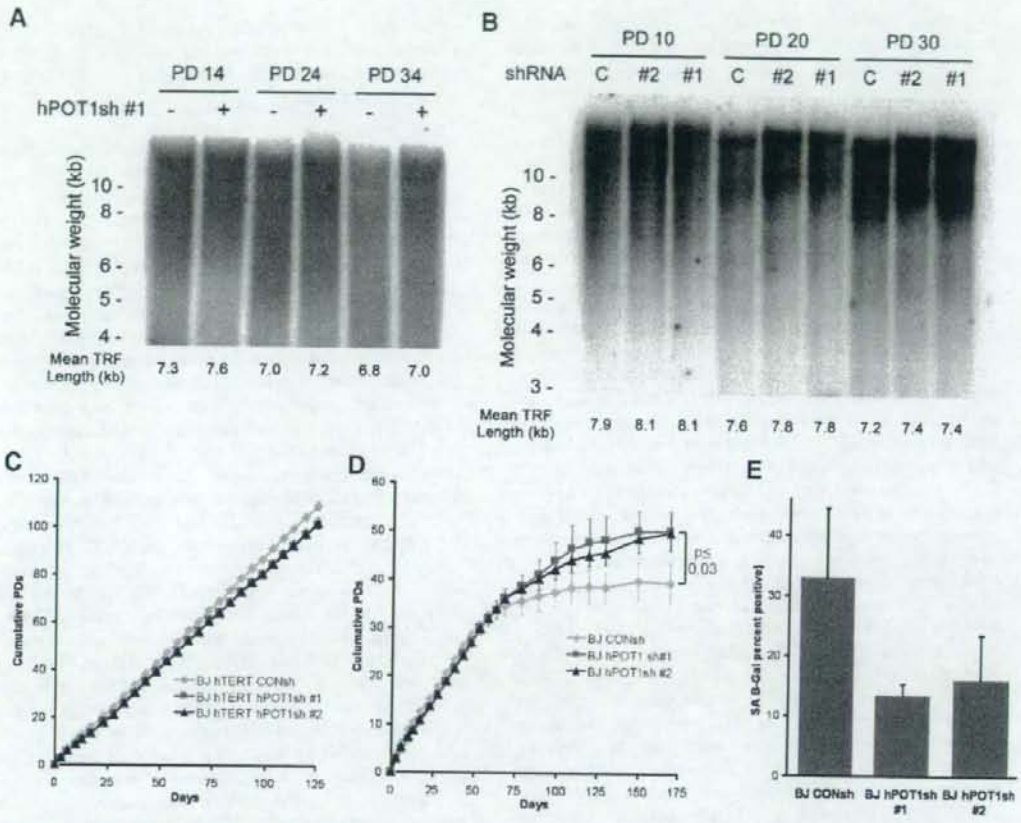

FIGURE 4. Long-term effects of *hPOT1* suppression on telomere length and replicative senescence. **A.** TRF Southern of BJ cells over a span of 34 PDs. BJ cells were infected with a control hairpin (−) or an hPOT1 hairpin (+) and DNA collected at the indicated mean PD after infection. BJ cells used in this experiment are of a lower initial starting PD from those in Figs. 1 and 2. The mean TRF length for each sample is indicated beneath the corresponding lane. Left, DNA size markers in kb. **B.** TRF Southern of HFF cells over a span of 30 PDs. HFF cells were infected with a control hairpin (*C*) or one of two *hPOT1*-specific hairpins (*#1* or *#2*) and DNA was collected at the indicated mean PD after infection. The mean TRF length for each sample is indicated beneath the corresponding lane. Left, DNA size markers in kb. **C.** Long-term proliferation of BJ hTERT cells after *hPOT1* suppression. BJ hTERT cells were infected with a control hairpin (*CONsh*) or one of two hPOT1 hairpins (*hPOT1 #1* or *hPOT1 #2*). Cumulative PD measurements represent an average of three separate cultures. **D.** Long-term proliferation of BJ cells after *hPOT1* suppression. BJ cells were infected with CONsh or hPOT1 #1 or hPOT1 #2. Cumulative PD measurements represent an average of three separate cultures and the *P* value (two-tailed *t* test) indicates the degree of statistical significance between the pairwise comparison of CONsh and either hPOT1sh #1 or hPOT1sh #2 ($P \leq 0.03$, for both comparisons). **E.** SA β-gal staining. Values represent the percentage of positively staining cells of at least 100 total cells scored in triplicate of cells from day 69 of the proliferation experiment shown in **D.**

of telomerase by DN-hTERT diminished the increase in telomere length seen after hPOT1sh #1 introduction by 50% to 100% as assessed by TRF length Southern blotting (Fig. 5C) and correlates with results obtained in BJ cells using quantitative FISH (Fig. 5D). These observations indicate that the telomere elongation observed after *hPOT1* suppression depends on the presence of telomerase.

Discussion

Telomere Length Control by hPOT1

Prior reports have described the effects of perturbing *POT1* function on telomere length in murine, galline, and immortal human cells with constitutive telomerase expression (22, 25, 34, 35, 40). Here, we investigated the effects of suppressing *hPOT1* in normal human cells where telomerase activity is tightly regulated and telomeric DNA is lost with each round of cell division, a situation that represents normal human cells. We had previously shown that hTERT is expressed in normal human fibroblasts in an S-phase–restricted manner but that this S-phase–regulated telomerase does not affect overall telomere length (8). Therefore, it is unclear whether the inability of hTERT to maintain telomere length is because this low level of hTERT is not competent to act on telomeres or because of a suppressive mechanism inhibiting telomerase in these cells. Studies in *Saccharomyces cerevisiae* further suggest that telomere elongation by telomerase is dependent on telomere length and binding to Rif1 and Rif2 (20) or binding to Rap1p

(41). These observations have led to the view that S-phase telomerase is restricted from elongating telomeres in mortal human cells due to a repressive mechanism located at the telomere.

Here, we present evidence that suppression of *hPOT1* expression by shRNA in mortal diploid human cells altered normal telomere attrition, resulting in a larger mean telomere length in cells in which *hPOT1* has been suppressed. This change in telomere attrition occurred shortly after *hPOT1* suppression, resulting in telomere maintenance at a new set point. Once this new set point was reached, telomere attrition continued to occur at a normal rate with subsequent successive cell divisions.

We and others (22, 23, 25) have observed that suppression of *hPOT1* in immortal cells that express telomerase constitutively leads to an increase in telomere length beyond the normally maintained set point. Here, we find that simultaneous overexpression of *hTERT* and suppression of *hPOT1* in mortal BJ cells results in the combined effect of telomere elongation expected after *hTERT* overexpression in primary cells and the additional increase in telomere length noted after *hPOT1* suppression. However, we noted neither a synergistic nor epistatic relationship between *hTERT* overexpression and *hPOT1* suppression, suggesting that these manipulations may affect telomere length and/or structure in separate, noncomplementary ways.

In normal human fibroblasts that express low levels of hTERT in S phase, we observed that the increase in mean telomere length seen after *hPOT1* suppression can be blunted by suppression of *hTERT* or inhibition of telomerase. These observations suggest that the S-phase–restricted hTERT present in normal human cells is competent to act on the telomere but is inhibited by an hPOT1-dependent suppressive mechanism. However, because we were unable to completely eliminate the telomere elongation phenotype seen in these cells by suppressing hTERT expression, it remains possible that hPOT1 also participates in hTERT-independent telomere replication. Indeed, an increase in homologous recombination has been observed on deletion of *POT1a* in mice (33), and this increased recombination activity may also help explain the telomere lengthening observed here.

Although this study is unique in its analysis of the effects of suppression of hPOT1 on telomere length and replicative senescence in primary human cells and the dependence of these effects on hTERT, our studies are consistent with prior studies in human, murine, and galline cells that constitutively express hTERT. Suppression of POT1 in telomerase-positive human (24, 25, 42) or galline cells (40) induces telomere elongation, and overexpression of an hPOT1 mutant lacking the 5′ oligonucleotide-binding fold domains leads to telomere elongation in immortal human cells (22, 26). However, others have found that hPOT1 overexpression in human cells that constitutively express hTERT can promote telomere elongation (23). Furthermore, in mice, two groups have found both telomere elongation (34) or no change in overall telomere length (35) after germ-line deletion of *POT1a*, whereas targeted deletion of *POT1b* results in mTERC-independent 3′ overhang lengthening (35). These manuscripts represent a growing body of literature supporting the notion that POT1 functions in telomere 3′ overhang protection, telomeric DNA damage signaling, and cell cycle progression. However because many of the conclusions about POT1 function vary depending on the model system used, we believe that studies in primary human cells are well positioned for understanding the role of hPOT1 in normal human biology.

Contributions to Replicative and Stress-Induced Senescence

Human cells that undergo extensive passage *in vitro* eventually enter a metabolically active yet growth-arrested state termed replicative senescence (43). In normal human cells, telomere attrition occurs with serial passage (9) and has been suggested to trigger the onset of replicative senescence (11). We found that suppression of *hPOT1* in early-passage BJ fibroblasts resulted in a population of cells with a longer mean telomere length that correlates with an increase in the number of PD required to reach replicative senescence.

Human cells can also be induced to enter senescence acutely by exposure to stresses such as oncogenic RAS (44), hydrogen peroxide (45), and X-ray irradiation (46). Moreover, when human cells reach replicative senescence, DNA damage response factors accumulate at telomeres in telomere TIFs (47, 48). Suppression of *hPOT1* in human fibroblasts induces TIF formation acutely in both primary and hTERT-overexpressing cells but has been shown to induce ATR-dependent senescence only in primary cells (38, 40, 42, 49, 50). Here, we show that the impairment of cell proliferation seen with *hPOT1* suppression correlates with the proliferative history of primary BJ and HFF cells. Indeed, suppression of *hPOT1* only induces senescence acutely in fibroblasts that have undergone a considerable number of PDs. These observations are consistent with recent reports implicating proliferative age and/or levels of p16, which rise with passage, as key factors in the competency of cells to undergo acute senescence programs (51, 52). Alternatively, it is also possible that changes in telomere structure occur with successive passage that alters the response to suppression of *hPOT1*. In this case, one might expect that late-passage cells are more dependent on hPOT1 for telomere end protection and acutely enter senescence in its absence. Indeed, although we observed induction of TIFs on *hPOT1* suppression in both early- and late-passage cells, we detected DNA bridges only in later-passage cells. These data suggest that early-passage cells are able to tolerate or compensate for reduced hPOT1 expression, whereas in later-passage cells suppression of *hPOT1* results in telomeric damage and the onset of senescence. However, given the number of stimuli that are acting on any given cell, a combination of telomeric and nontelomeric stresses may contribute to the senescence phenotype seen here.

Regulation of the telomere and induction of senescence are emerging as key processes underlying our ability to understand the development of cancer and the process of aging. The recent identification of senescent cells in premalignant and malignant human tissue highlights the importance of understanding the contributions of senescence to the suppression or progression of the malignant state (53). Telomeric stability and proper control of telomere length both are important in determining whether a cell enters the senescent state and are fundamental functional acquisitions found in cancer.

The multiple effects of suppression of *hPOT1* on telomere length control, cellular proliferation, induction of senescence,

and the timing of the onset of replicative senescence provide additional insight into the interplay between telomere biochemistry and the senescence program. One approach to target telomeres involves agents that act by stabilizing G-quadruplex structures (54). Telomeric G-quadruplexes introduce kinks in telomeric DNA and inhibit telomere elongation; therefore, stabilization of G-quadruplexes would be expected to limit cell growth (55, 56). Biochemical studies show that hPOT1 can enhance the ability of G-quadruplex telomeric DNA to act as a telomerase substrate *in vitro* (30). Taken